

UNCLASSIFIED
RESTRICTED

Copy No.

5

RM No. L8E18



3 1176 00096 1871

NACA RM No. L8E18

To UNCLASSIFIED ~~RESTRICTED~~ **NACA**

By authority of *J. W. Crowley* Date *10-29-53*
per NACA Release form #1545. By HSTR, 7-17-53.

RESEARCH MEMORANDUM

THE EFFECT OF BOUNDARY-LAYER CONTROL BY SUCTION AND SEVERAL
HIGH-LIFT DEVICES ON THE LONGITUDINAL AERODYNAMIC
CHARACTERISTICS OF A 47.5° SWEEPBACK
WING-FUSELAGE COMBINATION

By

Jerome Pasamanick and Anthony J. Proterra

Langley Aeronautical Laboratory
Langley Field, Va.

CLASSIFIED DOCUMENT

This document contains classified information affecting the National Defense of the United States within the meaning of the Espionage Act, USC 50-31 and 32. Its transmission or the revelation of its contents in any manner to an unauthorized person is prohibited by law. Information so classified may be imparted only to persons in the military and naval services of the United States, appropriate civilian officers and employees of the Federal Government who have a legitimate interest therein, and to United States citizens of known loyalty and discretion who of necessity must be informed thereof.

NATIONAL ADVISORY COMMITTEE FOR AERONAUTICS

WASHINGTON
November 4, 1948

~~RESTRICTED~~

UNCLASSIFIED

NATIONAL ADVISORY COMMITTEE FOR AERONAUTICS

RESEARCH MEMORANDUM

THE EFFECT OF BOUNDARY-LAYER CONTROL BY SUCTION AND SEVERAL
HIGH-LIFT DEVICES ON THE LONGITUDINAL AERODYNAMIC
CHARACTERISTICS OF A 47.5° SWEEPBACK
WING-FUSELAGE COMBINATION

By Jerome Pasamanick and Anthony J. Proterra

SUMMARY

An investigation has been made in the Langley full-scale tunnel of a 47.5° sweptback wing-fuselage combination equipped for boundary-layer control by suction. The wing section was NACA 64₁-All2 normal to the quarter-chord line, the aspect ratio was 3.5, and the taper ratio was 0.5. The wing configurations tested included the wing with various combinations of extensible leading-edge and split flaps.

Increasing the Reynolds number from 2.1×10^6 to 7.1×10^6 and 2.1×10^6 to 5.0×10^6 had no appreciable effect on the lift and drag characteristics of the plain wing and the wing with semispan split flaps, respectively. The increase in Reynolds number, however, caused a destabilizing shift of the linear portion of the pitching-moment curve and progressively moved an unstable break in the curve near the stall to higher lift coefficients.

Combinations of slots utilizing the 0.20-percent-chord slot, are the most effective for boundary-layer control as initial separation occurred near the wing leading edge. Applying suction through the 0.70-chord slot was not effective in improving the wing characteristics.

The maximum lift coefficient of the plain wing was 0.96, 1.07, and 1.11 for suction flow coefficients of 0, 0.024, and 0.037, respectively. Boundary-layer control did not eliminate an unstable pitching-moment break that occurred near maximum lift.

Semispan and full-span split-flap deflection resulted in maximum lift coefficients of 1.02 and 1.09, respectively. Applying a suction flow coefficient of 0.037 increased the corresponding maximum lift coefficients to 1.14 and 1.23. With and without boundary-layer control the model was longitudinally unstable at the stall.

The application of boundary-layer suction with the 0.50-, 0.60-, and 0.71-semispan extensible leading-edge flap configurations produced maximum lift coefficients of 1.14, 1.17, and 1.18, respectively. Without

boundary-layer control the model configurations were longitudinally unstable at the stall. However, applying suction at flow coefficients of both 0.024 and 0.037 to the 0.50- and 0.60-semispan leading-edge flap configurations resulted in longitudinal stability at the stall.

With the semispan split flaps in combination with the extensible leading-edge flaps the highest maximum lift coefficient (1.28) was obtained for the 0.71-semispan leading-edge flap configuration at a suction flow coefficient of 0.037. All combinations of split- and leading-edge-type flaps resulted in longitudinal instability at the stall with and without boundary-layer control.

Changing the wing-tip shape from a round to a square tip had only minor effects on the lift and drag characteristics of the model. The pitching-moment characteristics were improved for the 0.50-semispan extensible leading-edge flaps with and without suction. No appreciable changes occurred for the other flap configurations.

Boundary-layer control produced a trend toward the reduction of the measured drag coefficients in the higher lift-coefficient range and did not appreciably change the measured drag coefficients in the low lift-coefficient range. For the plain wing the drag coefficient equivalent to the blower power required to discharge the boundary layer at free-stream total head is approximately 0.039 and 0.102 for flow coefficients of 0.024 and 0.037, respectively.

Blower-power failure would result in a reduction in the maximum lift coefficient and would also result in an abrupt longitudinal instability at the lower maximum lift coefficient.

INTRODUCTION

The recent design trend toward the use of thin highly sweptback wings for high-speed flight has greatly emphasized the necessity for determining means whereby the low-speed characteristics of such wings can be improved. A study has been made with the use of leading- and trailing-edge high-lift devices of methods designed to eliminate wing-tip stall and to increase the maximum lift of sweptback wings (reference 1). It was shown in the early investigations of sweptback wings that the flow of the boundary layer contributed largely to the poor longitudinal low-speed characteristics. An investigation was initiated at the Langley full-scale tunnel to determine the effect of boundary-layer control by suction on the aerodynamic characteristics of a sweptback wing. The sweepback of the wing was 47.5° , the aspect ratio was 3.5, the taper ratio was 0.5, and the airfoil sections normal to the quarter-chord line were NACA 64₁-A112. The wing panels were mounted in a low midwing position on a circular fuselage.

Boundary-layer control was applied through suction slots located at the 0.20-, 0.40-, and 0.70-chord spanwise stations on the outboard

half of each wing panel. Additional high-lift devices tested in conjunction with the plain wing consisted of full-span and semispan split flaps and partial-span extensible leading-edge flaps.

The results contained herein present the effect of boundary-layer control on the maximum lift and longitudinal stability characteristics of the model at zero yaw. Forces and moments were measured for each configuration tested with and without suction for a range of angle of attack through the stall. Reynolds number effects with the slots sealed have been determined for the plain wing and for the wing with semispan split flaps from 2.1 to 7.1×10^6 , respectively. All other configurations were tested at a Reynolds number of 4.2×10^6 corresponding to a Mach number of approximately 0.07 . The results of the effect of boundary-layer control on the aerodynamic characteristics of the model in yaw are presented in reference 2.

COEFFICIENTS AND SYMBOLS

All results are presented in standard NACA form of coefficients, forces, and moments and are referred to the wind axes. Moments are referred to the quarter-chord point of the mean aerodynamic chord.

C_L lift coefficient (L/qS)

C_D measured drag coefficient (D/qS)

C_{DE} drag coefficient equivalent to blower power $\left(\frac{C_P C_Q S'}{\eta} \right)$

C_m pitching-moment coefficient (M/qSc)

C_Q suction flow coefficient (Q/VS')

C_p pressure coefficient $\left(\frac{H - H_d}{q} \right)$

η internal ducting and blower efficiency

R Reynolds number ($\rho Vc/\mu$)

L lift, pounds

D measured drag, pounds

M pitching moment, positive when moment tends to increase angle of attack, foot-pounds

q free-stream dynamic pressure, pounds per square foot $\left(\frac{1}{2} \rho V^2 \right)$

- ρ mass density of air, pounds-second² per foot⁴
- V free-stream velocity, feet per second
- S total wing area, feet²
- S' wing area affected by suction slots, feet²
- c wing chord, measured in plane perpendicular to quarter-chord line, feet
- c' wing chord, measured in plane parallel to plane of symmetry, feet
- \bar{c} wing mean aerodynamic chord, measured in plane parallel to plane of symmetry, feet $\left(\frac{2}{S} \int_0^{b/2} c'^2 db \right)$
- b wing span, feet
- Q total air quantity removed through suction slots, feet³ per second
- H free-stream total pressure, pounds per foot²
- H_d total pressure inside wing duct, pounds per foot²
- μ coefficient of viscosity, pounds-second per foot²
- α angle of attack of wing chord line, measured in plane of symmetry, degrees

MODEL

A three-view drawing showing the principal dimensions of the model is given in figure 1, and figure 2 shows the model mounted in the Langley full-scale tunnel. The wing leading-edge sweepback was 47.5° and the sweepback of the quarter-chord line was 45°. The airfoil sections normal to the quarter-chord line were NACA 64₁-All₂, and the maximum thickness and station of maximum thickness in the plane of symmetry was 0.09c' and 0.44c', respectively. There was no geometric dihedral or twist and the wing panels were mounted on a circular fuselage in a low midwing position at zero incidence with respect to the fuselage center line.

The wing tip was rounded in both plan form and cross section (figs. 3(a) and 3(b)), and a square tip (figs. 3(a) and 3(b)) was installed during the latter part of the test program. The square tip increased the wing area from 229.4 to 231 square feet without changing the span or the taper ratio of the wing.

A schematic drawing showing cutaways of the wing panel and fuselage is given in figure 4. The wing panels were of a box-beam-type construction and the wing skin was constructed of laminated mahogany surfaced and finished to the required section. Slots 0.01c wide were located at the 0.20c, 0.40c, and 0.70c stations on the outboard half of each wing panel. The wing area affected by the suction slots was 83.8 feet². A cross section showing the location and detail dimensions of the slots are given in figures 3(c) and 3(e), respectively.

The fuselage which housed the boundary-layer blower equipment had a fineness ratio of 9.35:1. The axial-flow single-stage blower was coupled to a variable-speed electric motor and the installation inside the fuselage is shown in figure 4.

Four pitot-static tubes located 90° apart in the annulus ahead of the fan were used to determine the total flow quantity passing through the suction slots. The slot and wing-duct losses were measured by total-pressure tubes located at the wing-fuselage junction in each wing panel. The location of the instrumentation is shown in figure 4.

The installations and locations of the auxiliary high-lift devices used in combination with the plain wing are shown in figure 3(a). The dimensions and deflection angles of the split- and extensible leading-edge-type flaps are given in figures 3(d) and 3(c), respectively. The 0.20c' semispan split flaps extended outward from the fuselage to the $0.55\frac{b}{2}$ station and the 0.20c' full-span split flaps extended outward to the $0.88\frac{b}{2}$ station. The 0.10c' extensible leading-edge flaps were $0.50\frac{b}{2}$, $0.60\frac{b}{2}$, and $0.71\frac{b}{2}$ -span and extended outward to the $0.92\frac{b}{2}$ station for the rounded-tip wing and to the $1.0\frac{b}{2}$ station for the square-tip wing. Each flap was constructed from thin sheet metal and was faired to the wing contour at the surface of attachment.

The model was sanded and lacquered to provide very smooth surfaces and the main construction was sufficiently rigid to reduce deflections to a minimum.

TESTS AND METHODS

In order to determine the effect of suction-slot location on the flow over the wing, extensive exploratory tests were made of the wing with and without split flaps for a large number of slot arrangements. The configurations were such that the slots were tested separately, in combination with one another, and in partial spanwise sections. Force tests and flow observations of wing upper-surface tufts were made over a large angle-of-attack range at suction flow coefficients of 0.024 and 0.037 at a Reynolds number of 4.2×10^6 . The lift and drag data as determined from these studies with the tufts attached to the wing are suitable as qualitative results. The pitching-moment data may have some scatter but is sufficiently accurate to indicate the longitudinal stability characteristics of the wing.

A list of the test configurations is given in table I. Reynolds number effects for the wing with round tips and with the slots sealed were determined for the plain wing and for the wing with semispan split flaps from 2.1 to 7.1×10^6 and 2.1 to 5.0×10^6 , respectively. Except where noted otherwise, the data are for a Reynolds number of 4.2×10^6 and for flow coefficients of 0.024 and 0.037 . The results for the zero flow coefficient $C_q = 0$ represent the condition having the slots sealed and faired to a smooth contour with the wing. A few tests were made to determine the effect of sudden loss of boundary-layer suction caused by a power failure by having the slots open and allowing the fan to windmill.

The stalling characteristics of the wing were determined by observing the behavior of wool tufts attached to the upper surface of the wing. The tufts were located approximately at the $0.26c$, $0.46c$, and $0.76c$ stations and were spaced approximately 12 inches apart along the span.

All of the test results have been corrected for jet-boundary effects, blocking effects, stream alinement, and wing-support interference. In addition, a drag tare correction has been applied to compensate for the effect of the air-jet thrust due to the fan operation. The drag coefficients as presented in the data figures are measured drag coefficients and do not include the blower-power drag coefficients.

DISCUSSION OF RESULTS

Characteristics of the Wing with Rounded Tips

Reynolds number effect.- The effect of Reynolds number on the longitudinal aerodynamic characteristics of the wing with and without semispan split flaps and without boundary-layer control is shown in figure 5. The maximum lift coefficient for the plain wing increases slightly (about 0.04) between Reynolds numbers of 4.2×10^6 and 6.1×10^6 whereas for the flapped wing, an increase in $C_{L_{max}}$ of about 0.05 occurs between values of 2.9×10^6 and 4.2×10^6 . The lift peaks for the plain wing are smooth and rounded and the slope of the lift curve gradually decreases after maximum lift, the peaks for the flapped wing are also rounded but the lift curve remains practically constant beyond the point of maximum lift.

The lift and drag characteristics are not materially changed at the higher Reynolds numbers; however, there is an appreciable influence of Reynolds number on the pitching-moment characteristics for the plain and flapped wing configurations. With increasing Reynolds number there is a destabilizing shift of the linear portion of the pitching-moment curve and of considerable importance is the delay of the unstable break of the pitching-moment curve to higher lift coefficients. From the trend

of data shown it is highly possible that the instability occurring at high lift coefficients may be eliminated at Reynolds number greater than 7.1×10^6 . In all cases, the sudden instability is closely related to the point on the lift curve where initial stall occurs and where the drag-coefficient curve slope suddenly increases. The delay of the instability to higher lift coefficients with increasing Reynolds number is attributed to an improvement in the flow of the boundary layer, thereby delaying the tip stall and the rapid forward shift of the center of pressure.

Results with the full-span split flaps did not differ basically from the configuration of the semispan flaps and therefore are not presented.

Preliminary slot investigation.- In order to determine the effect of boundary-layer-suction slot location on the aerodynamic characteristics of the wing, a preliminary investigation of configurations using individual slots and multiple slot combinations was made. The results of this investigation are given in figure 6 for a Reynolds number of 4.2×10^6 and an angle-of-attack range from 12° to the angle of maximum lift at several suction flow coefficients. Additional tests were made with different percent spanwise lengths of slots but these results were found to be essentially the same as those of figure 6 and therefore are not shown. Either the 0.20c slot alone or in combinations using that slot as shown in figure 6 gave the best results for a flow coefficient of 0.024. An increase in C_Q from 0.024 to 0.033 for the 0.20c slot combinations resulted in increases in $C_{L_{max}}$ of the order of 0.04. Neither location nor suction at flow coefficients above 0.024 had any appreciable effect on the drag of the model. The unstable break in the pitching-moment curve that occurred for the basic wing was not eliminated by boundary-layer suction for any of the slot arrangements tested. The test program that followed this preliminary investigation was completed using all three slots, although the results in figure 6 show that suction through the 0.70c slot was ineffective.

In order to present conditions at a given flow coefficient, a portion of the data presented in the paper was obtained by cross-plotting curves of C_L , C_D , and C_m against C_Q for constant angle of attack.

Characteristics of the plain wing.- The characteristics of the plain wing (fig. 7) show that the maximum lift coefficient without boundary-layer control was 0.96 at an angle of attack of 21° . The pitching moment was neutrally stable up to a lift coefficient of approximately 0.55 and stable from thereon to C_L of 0.90. At a C_L of 0.90, which was below the maximum lift, there was a severe unstable pitching moment and beyond this lift coefficient the lift-curve slope decreased and the drag rapidly increased. The tuft diagram, figure 8 in conjunction with figure 7, indicates that up to a C_L of 0.55 the disturbed flow at the trailing edge of the tip had little or no effect upon the location of the center of pressure. In the range of C_L from 0.55 to 0.90 the

region of disturbed flow increased and caused a strong outward flow of the boundary layer along the rear 0.30c lines of the wing. At a C_L of 0.90 the tips were intermittently stalled and the flow over the wing area behind the moment center was very unsteady.

The application of boundary-layer suction at flow coefficients of 0.024 and 0.037 increased the maximum lift to 1.07 and 1.11, respectively. The increase in maximum lift due to suction was obtained by the clean-up of the flow in the region of the slots which resulted in a slight increase in the lift-curve slope and an extension of the linear portion of the lift curve to higher angles of attack. Up to moderate lift coefficients, the flow over the region covered by the slots was greatly improved, but the flow pattern at the tips was similar to that for the sealed condition. With boundary-layer suction there was a reduction in the spanwise flow of the boundary layer in the region behind the suction slots. The longitudinal stability was improved by suction as a result of the delay in the forward shift of the center of pressure; however, the unstable break near the maximum lift was not eliminated.

Characteristics of the wing with split flaps.- The wing with semi-span and full-span split flaps gave maximum lift coefficients of 1.02 and 1.09, respectively, for the slot sealed condition (fig. 9). These values of $C_{L_{max}}$ are 0.06 and 0.13 higher than that measured for the plain wing. For these flapped configurations the lift increments below the stall calculated using the simple sweep theory (reference 3) are in good agreement with the results presented herein. With boundary-layer suction at a C_q of 0.024 the maximum lift coefficient was increased to 1.09 and 1.06 for the two flapped conditions. Increasing C_q to 0.037 resulted in a further increase in $C_{L_{max}}$ to 1.14 for the semispan flapped wing and 1.23 for the wing with full-span flaps. The pitching-moment curves for both flap configurations indicate the same trend of stability as the plain wing with and without suction particularly as regards the longitudinal instability at the stall. Tuft studies of the semispan flapped wing with and without boundary-layer suction (fig. 10) show the early tip stall and flow patterns to be typical of that for the plain wing.

Characteristics of the wing with extensible leading-edge flaps.- The plain wing and the wing with split-flap results have shown that the stalling characteristics are essentially unaffected by boundary-layer control. A two-dimensional-flow investigation of the NACA 64₁-A112 airfoil section indicated the stall to be characterized by the tendency for separation to occur first at the leading edge. A simple device available for eliminating the flow breakdown at the leading edge is an extensible leading-edge flap which in effect modifies the airfoil contour. This type of flap has been shown to be an effective stall-control device on a wing of lower sweep at high Reynolds number (reference 1).

The results obtained for the extensible leading-edge flaps are shown in figure 11. The addition of the flaps extended the lift curve so that greater maximum lift occurred at slightly higher angles of attack than was observed for the plain wing, which results from the delay of leading-edge separation and in part from the effective increase in wing area. Without suction, the $0.50\frac{b}{2}$ -span, $0.60\frac{b}{2}$ -span, and $0.71\frac{b}{2}$ -span flaps increased the value of $C_{L_{max}}$ of the plain wing by approximately 0.14 in each case. The $0.50\frac{b}{2}$ -span flap configuration with suction at a C_Q of 0.024 produced only a small further increment, but the larger flaps each produced an increment of approximately 0.05 for a flow coefficient of 0.024. By increasing the suction coefficient to 0.037 an additional lift coefficient increment of approximately 0.03 was obtained for all three flap configurations, thus giving a maximum lift coefficient of 1.18 for the $0.71\frac{b}{2}$ -span flap.

The pitching-moment characteristics of the wing with extensible leading-edge flaps and without suction are similar to those of the plain wing. Approximately neutral longitudinal stability is shown over the low and medium range of C_L , and at higher lift coefficients there is an increase in stability followed by a sudden instability near the stall. The tuft studies of the wing with extensible leading-edge flaps (fig. 12) show that stall begins at the inboard end of the flap; whereas, for the plain wing stall first occurs at the wing tips. The initial stall at the inboard region is attributed to the disturbance created by the vortex shed from the end of the flap. Without suction the stall spreads rapidly outboard resulting in a forward movement in center of pressure with the ultimate longitudinal instability.

Application of a suction flow coefficient of 0.024 to both the $0.50\frac{b}{2}$ -span and $0.60\frac{b}{2}$ -span flap configurations resulted in a clean up of the flow behind the flaps with a slight instability occurring prior to the stable pitching moment at the stall (fig. 11). A further increase in the suction flow coefficient to 0.037 completely eliminated the slight instability with only the portion of the wing affected by the flap vortex being disturbed. Boundary-layer suction did not eliminate the instability at maximum lift for the $0.71\frac{b}{2}$ -span flap installation. Similar effects of the leading-edge flaps on the longitudinal characteristics have been shown on another sweptback wing without boundary-layer control by suction in reference 1. Since the flow on the wing is greatly affected by the flaps there appears to be an optimum span for control of the longitudinal characteristics of the wing near the stall. When the flap span exceeds the optimum configuration, the flow over the outer wing portion assumes the characteristics as shown for the plain wing.

Characteristics of the wing with combinations of extensible leading-edge and semispan split flaps.— The combinations of extensible leading-edge and semispan split flaps produced a maximum lift coefficient of approximately 1.15 which is 0.19 greater than that obtained for the plain

wing (figs. 7 and 13). For these configurations without boundary-layer suction the wing is neutrally stable up to stall and unstable at the stall. The instability at $C_{L_{max}}$ is a result of the tip stall due to the induced flow by the deflection of the split flaps (fig. 14).

Boundary-layer control with a suction flow coefficient of 0.024 increased the $C_{L_{max}}$ to 1.19 for the $0.50\frac{b}{2}$ -span combinations and to 1.21 and 1.23 for the $0.60\frac{b}{2}$ -span and $0.71\frac{b}{2}$ -span leading-edge flap combinations, respectively. Increasing the flow coefficient to 0.037 increased the values of $C_{L_{max}}$ to 1.21, 1.24, and 1.28 for the $0.50\frac{b}{2}$ -span, $0.60\frac{b}{2}$ -span, and $0.71\frac{b}{2}$ -span leading-edge flap combinations, respectively. The wing is longitudinally unstable at the maximum lift coefficient for all flap combinations at a suction flow coefficient of 0.024 and 0.037. The flow diagrams (fig. 14), for $C_Q = 0.037$, indicate that the flow in the area behind the slots is undisturbed up to maximum lift and initial stall occurs at the inboard end of the leading-edge flap. Slightly below maximum lift the tip sections also became stalled. At maximum lift the entire area behind the suction slot suddenly stalled resulting in longitudinal instability.

Effect of power failure.— Boundary-layer control in conjunction with the high-lift devices increased the lift and for some configurations eliminated the longitudinal instability at the stall. In the event of suction-power failure for an airplane in the landing condition using any one of the wing configurations as presented in figures 7, 9(a), 11(a), and 13(a), the detrimental effects of having the suction slots open and fan windmilling are clearly shown. There is a reduction in $C_{L_{max}}$, about 0.10 to 0.20 depending upon the flap configuration, and also an increase in the destabilizing pitching-moment tendencies. The maximum lift coefficients attained for this condition are in all cases lower than those determined for the wing without suction. An interesting characteristic of this condition is that the drag of the model at low lift coefficients is essentially unaffected by the slots-open fan-inoperative condition.

Drag characteristics.— The variations of measured drag coefficient with and without boundary-layer control are given in figures 7, 9, 11, and 13. The drag coefficients as presented do not include blower-power drag coefficients. The addition of split flaps without suction gave large increments of drag whereas the leading-edge flaps increased the drag only 0.007 over the plain-wing drag coefficients. The application of boundary-layer control produced a trend toward the reduction of the measured drag coefficients in the higher lift-coefficient range. In the low and moderate lift-coefficient range for the two suction-flow conditions investigated there is no appreciable change in the measured drag coefficients over the slot-sealed condition. Although no appreciable drag reduction was shown at low lift coefficients, it is possible that an optimum configuration would result in some reduction in the measured drag coefficient as indicated by recent two-dimensional tests of a similar airfoil section.

In order to obtain the total drag coefficient with boundary-layer control, the drag coefficient equivalent to the power required to discharge the air removed from the boundary layer at free-stream total head must be included. The blower-power equivalent drag coefficient is determined from the relationship

$$C_{D_E} = \frac{C_p C_Q S^2}{\eta S}$$

The variation of the pressure coefficient C_p with angle of attack for the model with and without high-lift devices and for suction flow coefficients of 0.024 and 0.037 are presented in figure 15. Computations of the approximate magnitudes of the power equivalent drag coefficients using average values of C_p over the angle-of-attack range, give values of C_{D_E} of 0.039 and 0.102 for flow coefficients of 0.024 and 0.037, respectively, for the plain-wing configuration. These values are undoubtedly high as no attempt was made to reduce the internal losses. From these calculations, however, it is apparent that the blower-power drag is an important factor to be considered when boundary-layer control is applied and every attempt should be made to keep internal losses at a minimum. For the test setup used, however, a C_Q of 0.037 resulted in a blower drag coefficient which is approximately 20 percent of the total drag at $C_{L_{max}}$ and approximately 85 percent of the total drag of the model at low lift coefficients. The horsepower required for boundary-layer control can be estimated by multiplying the equivalent drag coefficient by the wing area and the applicable values of free-stream velocity and dynamic pressure.

Characteristics of the Wing with Square Tips

The lift and drag characteristics of the wing with square tips are essentially the same as those presented for the wing with round tips. A summary of the maximum lifts obtained is presented in table II. The pitching-moment characteristics of the wing with square tips (fig. 16) show that with the $0.50\frac{b}{2}$ -span extensible leading-edge flaps installed and without boundary-layer control, there is a stable pitching-moment break at maximum lift coefficient but preceded by a mild instability. The stable pitching moment at $C_{L_{max}}$ appears to be the result of the improved flow over the tips due to the fact that the outboard end of the flap was extended to the extreme tip. The stable break at $C_{L_{max}}$ did not occur for either the $0.60\frac{b}{2}$ -span and $0.71\frac{b}{2}$ -span leading-edge flaps and the stall progression was similar to that of the rounded-tip wing. Boundary-layer suction for flow coefficients of 0.024 and 0.037 for both the $0.50\frac{b}{2}$ -span and $0.60\frac{b}{2}$ -span leading-edge flaps completely eliminated the instability at $C_{L_{max}}$ and gave a stable pitching moment at $C_{L_{max}}$. However, for the $0.71\frac{b}{2}$ -span flaps boundary-layer control did not eliminate the longitudinal instability at the maximum lift coefficient.

SUMMARY OF RESULTS

The results of the investigation in the Langley full-scale tunnel of a 47.5° sweptback wing-fuselage combination equipped for boundary-layer control by suction with various high-lift devices are summarized as follows:

1. An increase in Reynolds number from 2.1×10^6 to 7.1×10^6 and from 2.1×10^6 to 5.0×10^6 for the plain wing and for the wing with semispan split flaps, respectively, caused a destabilizing shift of the linear portion of the pitching-moment curve and progressively moved an unstable break in the curve near the stall to higher lift coefficients. The increase in Reynolds number did not appreciably affect the lift and drag characteristics.
2. Combinations of slots utilizing the forward most slot, 0.20c, are the most effective for boundary-layer control as initial separation occurred near the wing leading edge. Applying suction through the 0.70c slot was not effective in improving the wing characteristics.
3. The maximum lift coefficient of the plain wing with the rounded tips and without boundary-layer control was 0.96. Boundary-layer suction for flow coefficients of 0.024 and 0.037 increased $C_{L_{max}}$ to values of 1.07 and 1.11, respectively, with suction through the 0.20c, 0.40c, and 0.70c slot combination.
4. Without boundary-layer suction maximum lift coefficients of 1.02 and 1.09 were obtained for the wing with semispan and full-span split flaps, respectively. With a suction flow coefficient of 0.037 for the corresponding flap configurations the maximum lift coefficients were 1.14 and 1.23. With and without boundary-layer control the model was unstable at the stall.
5. The application of boundary-layer suction with the $0.50\frac{b}{2}$ -span, $0.60\frac{b}{2}$ -span, and $0.71\frac{b}{2}$ -span extensible leading-edge flap configurations produced maximum lift coefficients of 1.14, 1.17, and 1.18, respectively, for the suction flow coefficient of 0.037. Suction at flow coefficients of 0.024 and 0.037 resulted in longitudinal stability at the stall for both the $0.50\frac{b}{2}$ -span and $0.60\frac{b}{2}$ -span flap configurations. The $0.71\frac{b}{2}$ -span flap configuration was unstable at the stall with and without boundary-layer control.
6. Combinations of $0.50\frac{b}{2}$ -span, $0.60\frac{b}{2}$ -span, and $0.71\frac{b}{2}$ -span leading-edge flaps with semispan split flaps gave the highest maximum lift coefficients of 1.21, 1.24, and 1.28, respectively, for the suction flow coefficient of 0.037. The model was longitudinally unstable at the stall for all configurations with and without boundary-layer control.

7. Changing the wing-tip shape from a round to a square tip had only minor effects on the lift and drag characteristics of the model. The longitudinal stability characteristics of the model were improved for the $0.50\frac{b}{2}$ -span extensible leading-edge flaps with and without suction. No appreciable changes in the longitudinal characteristics occurred for the other flap configurations.

8. Boundary-layer control produced a trend toward the reduction of the measured drag coefficients in the higher lift-coefficient range and did not appreciably change the measured drag coefficients in the low lift-coefficient range. For the plain wing the drag coefficient equivalent to the blower power required to discharge the boundary layer at free-stream total head is approximately 0.039 and 0.102 for values of C_Q of 0.024 and 0.037, respectively.

9. Blower-power failure would result in a reduction in the maximum lift coefficient and would also result in an abrupt longitudinal instability at the lower maximum lift coefficient.

Langley Aeronautical Laboratory
National Advisory Committee for Aeronautics
Langley Field, Va.

REFERENCES

1. Graham, Robert R., and Conner, D. William: Investigation of High-Lift and Stall-Control Devices on an NACA 64-Series 42° Sweptback Wing with and without Fuselage. NACA RM No. L7G09, 1947.
2. Pasamanick, Jerome: The Effect of Boundary-Layer Control by Suction and of Several High Lift Devices on the Aerodynamic Characteristics in Yaw of a 47.5° Sweptback Wing-Fuselage Combination. NACA RM No. L8E21, 1948.
3. McCormack, Gerald M., and Stevens, Victor I., Jr.: An Investigation of the Low-Speed Stability and Control Characteristics of Swept-Forward and Swept-Back Wings in the Ames 40- by 80-Foot Wind Tunnel. NACA RM No. A6K15, 1947.

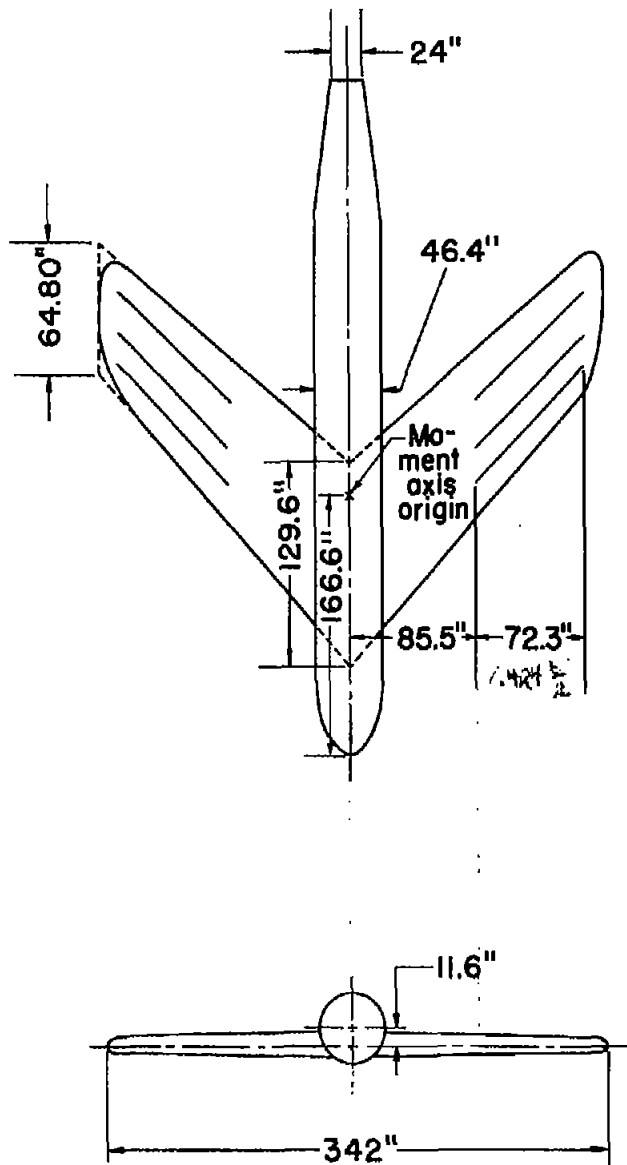
TABLE I.—PRESENTATION OF DATA

Type of data	Coefficients	Figure	Split flaps	Extensible leading-edge flaps, percent span	C_u	Remarks
Reynolds number effect Rounded tip	C_D , C_L , and C_M against α	5(a)	Off	Off	Slots sealed	α range, Reynolds number from 2.1 to 7.1×10^6
		5(b)	Semi-span	Off	Slots sealed	α range, Reynolds number from 2.1 to 5.0×10^6
Slot-location effect Rounded tip	C_D , C_L , and C_M against α	6	Off	Off	0.024, 0.037	α range from 12° to above maximum lift
Maximum lift Rounded tip	C_D , C_L , against α C_M against C_L	7	Off	Off	0, 0.024, 0.037	Fan inoperative α range
Tuft studies Rounded tip	-----	8	Off	Off	0, 0.037	α range
Maximum lift Rounded tip	C_D , C_L against α C_M against C_L	9(a)	Semi-span	Off	0, 0.024, 0.037	Fan inoperative α range
		9(b)	Full-span	Off	0, 0.024, 0.037	α range
Tuft studies Rounded tip	-----	10	Semi-span	Off	0, 0.037	α range
Maximum lift Rounded tip	C_D , C_L against α C_M against C_L	11(a)	Off	$0.50\frac{b}{2}$	0, 0.024, 0.037	Fan inoperative α range
		11(b)	Off	$0.60\frac{b}{2}$	0, 0.024, 0.037	α range
		11(c)	Off	$0.71\frac{b}{2}$	0, 0.024, 0.037	α range
Tuft studies Rounded tip	-----	12	Off	$0.50\frac{b}{2}$	0, 0.037	α range
Maximum lift Rounded tip	C_D , C_L against α C_M against C_L	13(a)	Semi-span	$0.50\frac{b}{2}$	0, 0.024, 0.037	Fan inoperative α range
		13(b)	Semi-span	$0.60\frac{b}{2}$	0, 0.024, 0.037	α range
		13(c)	Semi-span	$0.71\frac{b}{2}$	0, 0.024, 0.037	α range
Tuft studies Rounded tip	-----	14	Semi-span	$0.50\frac{b}{2}$	0, 0.037	α range
Pressure-coefficient curves Rounded tip	C_p against α	15	-----	-----	0.023, 0.037	Various flap configurations
Maximum lift Square tip	C_L , C_D against α C_M against C_L	16(a)	Off	off	0, 0.024, 0.037	α range
		16(b)	Off	$0.50\frac{b}{2}$	0, 0.024, 0.037	α range
		16(c)	Off	$0.60\frac{b}{2}$	0, 0.024, 0.037	α range
		16(d)	Off	$0.71\frac{b}{2}$	0, 0.024, 0.037	α range

TABLE II.- SUMMARY OF MAXIMUM-LIFT RESULTS

Configuration					$C_{L_{max}}$			$\Delta C_{L_{max}}$ due to suction	
Split flaps		Extensible leading-edge flaps			$C_q = 0$ slots, sealed and faired	$C_q = 0.024$	$C_q = 0.037$	$C_q = 0.024$	$C_q = 0.037$
Semi-span	Full-span	$0.50\frac{h}{2}$	$0.60\frac{h}{2}$	$0.71\frac{h}{2}$					
Rounded-tip wing									
					0.96	1.07	1.11	0.11	0.15
X					1.02	1.09	1.14	.07	.12
	X				1.09	1.16	1.23	.07	.14
		X			1.10	1.12	1.14	.02	.04
			X		1.09	1.13	1.17	.04	.08
				X	1.10	1.15	1.18	.05	.08
X		X			1.15	1.19	1.21	.04	.06
X			X		1.14	1.21	1.24	.07	.10
X				X	1.15	1.23	1.28	.08	.13
Square-tip wing									
					0.96	1.07	1.11	0.11	0.15
X					.99	1.07	1.13	.08	.14
		X			1.06	1.12	1.14	.06	.08
			X		1.07	1.13	1.16	.06	.09
				X	1.08	1.13	1.17	.05	.09
X		X			1.13	1.18	1.22	.05	.09
X			X		1.12	1.18	1.22	.06	.10
X				X	1.15	1.21	1.25	.06	.10





Total wing area:

Rounded tip 229.4 sq. ft.

Square tip 231.0 sq. ft.

Aspect ratio 3.5

Taper ratio 0.5

Airfoil section NACA 64₁-A112

Root chord 10.8 ft

Tip chord 5.4 ft

\bar{c} 8.37 ft

Figure 1.- Three-view drawing of a 47.5° sweptback wing-fuselage combination with boundary-layer control.

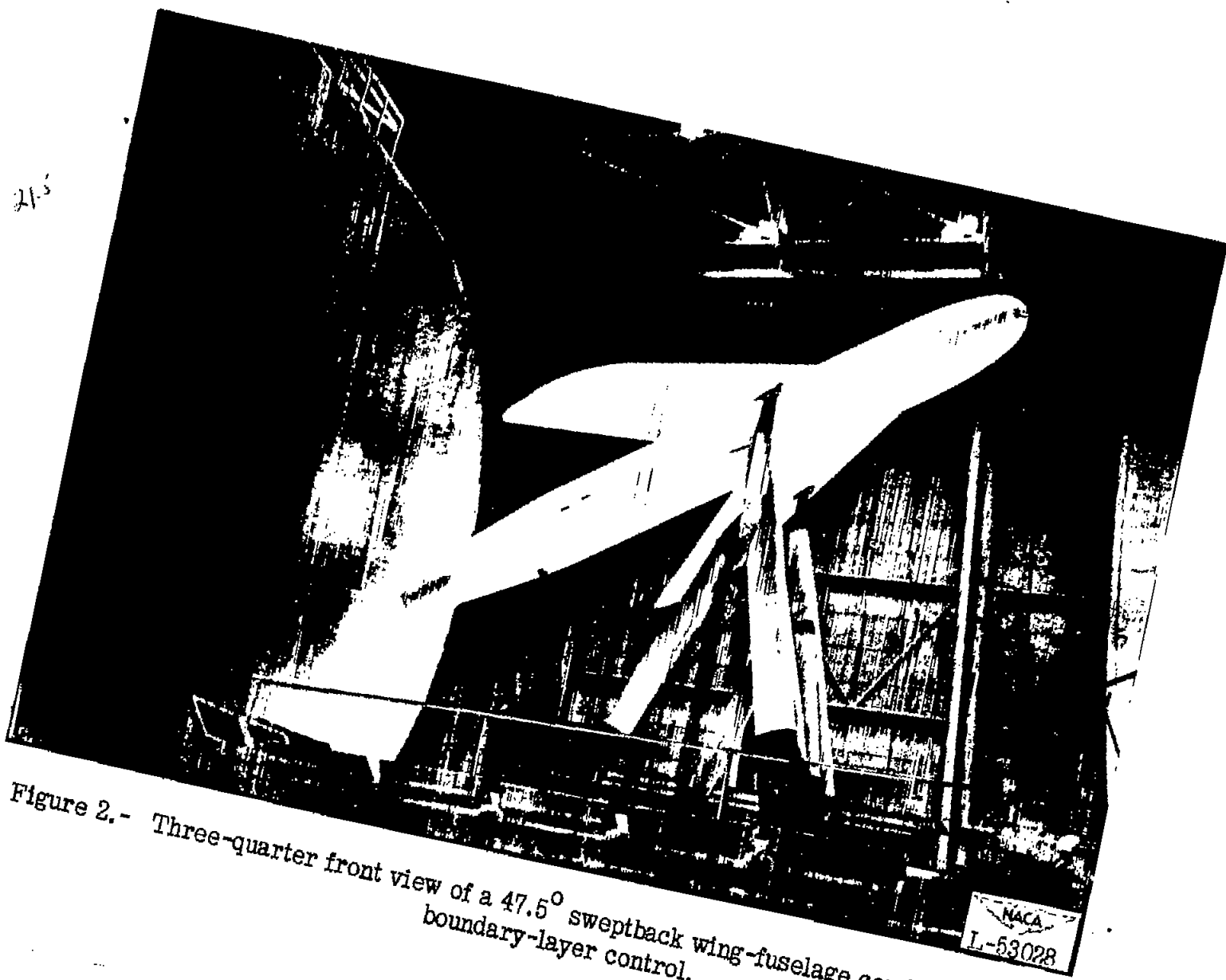
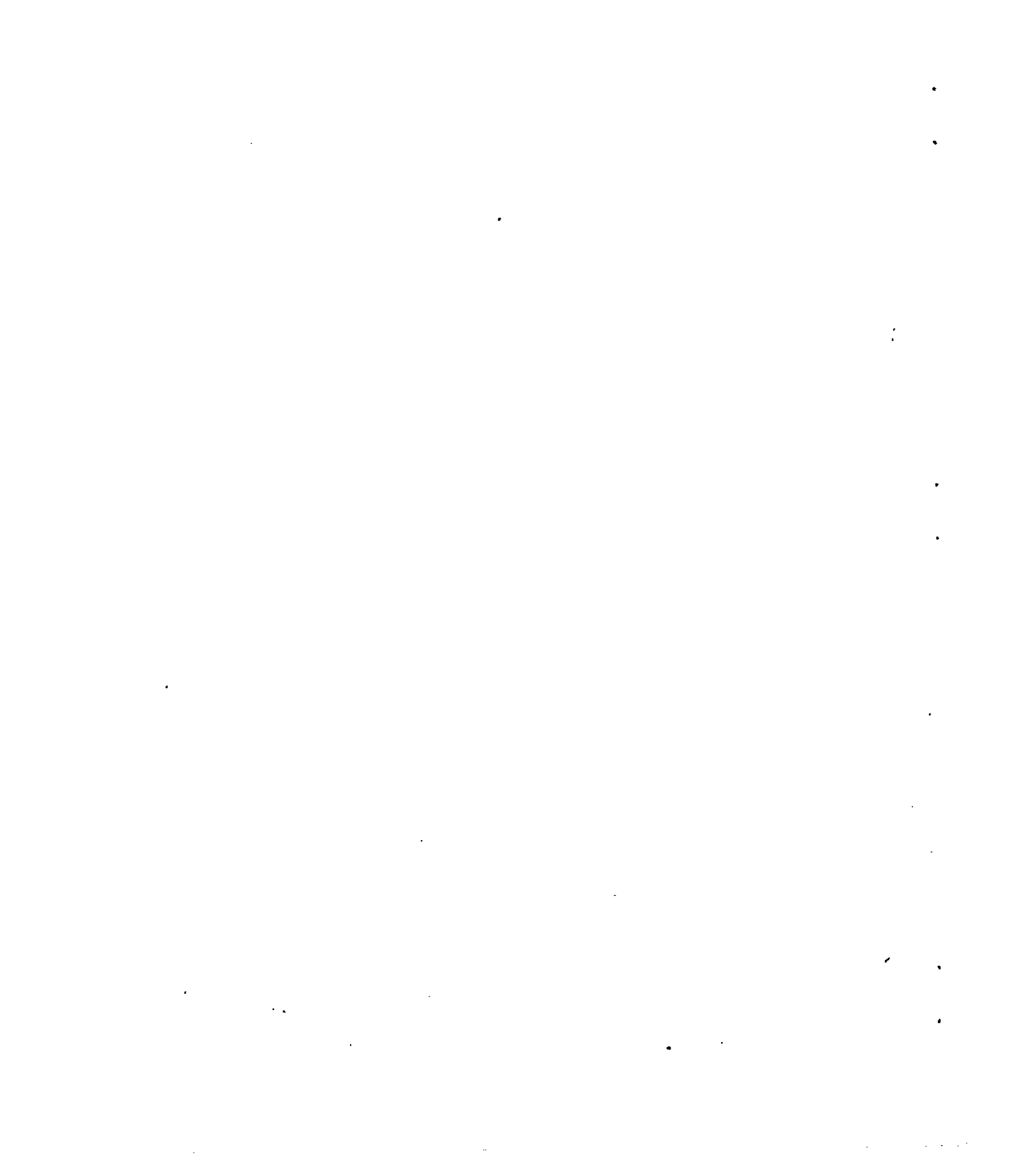


Figure 2.- Three-quarter front view of a 47.5° sweptback wing-fuselage combination with boundary-layer control.



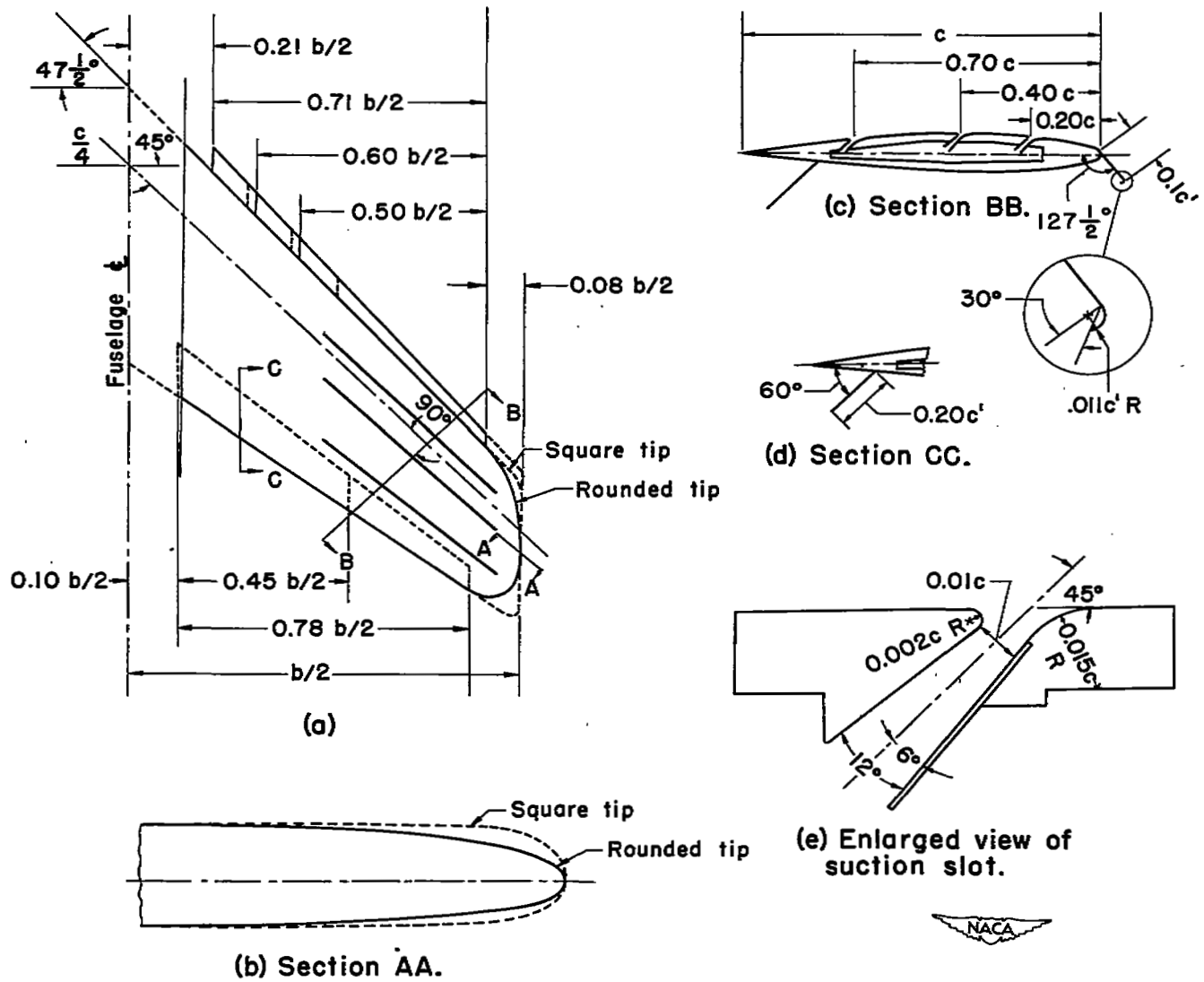


Figure 3.- The location and detail dimensions of high-lift devices.





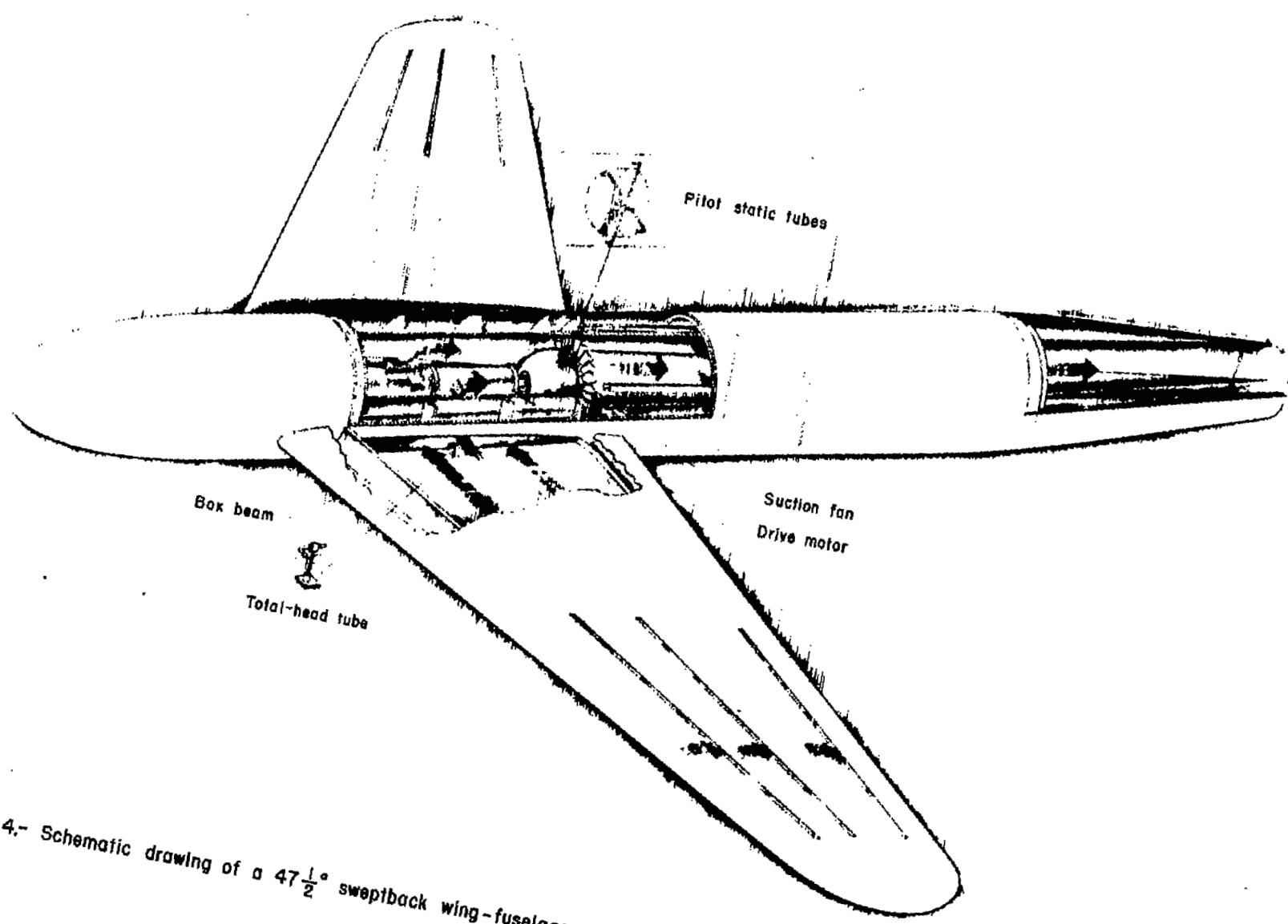
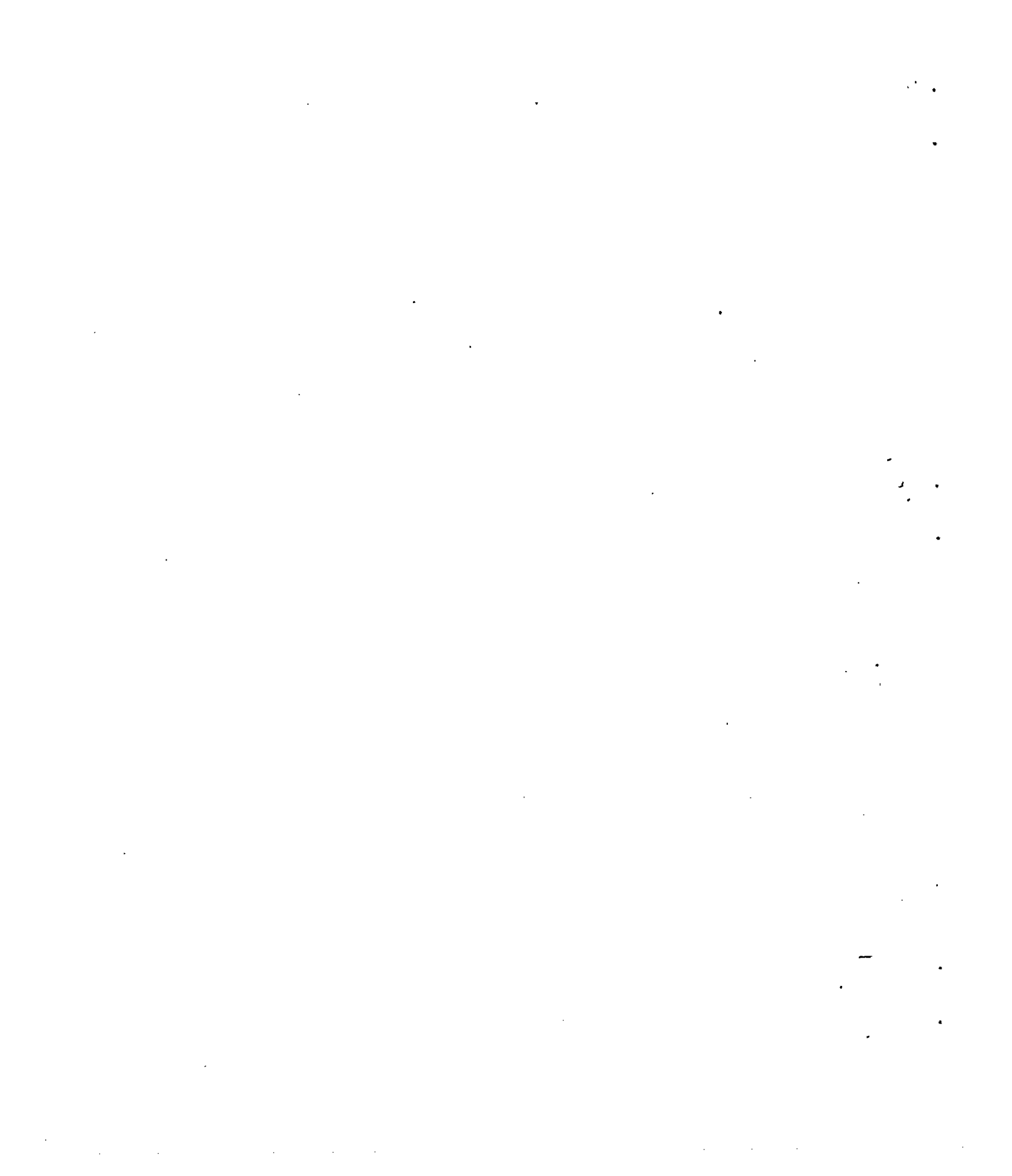
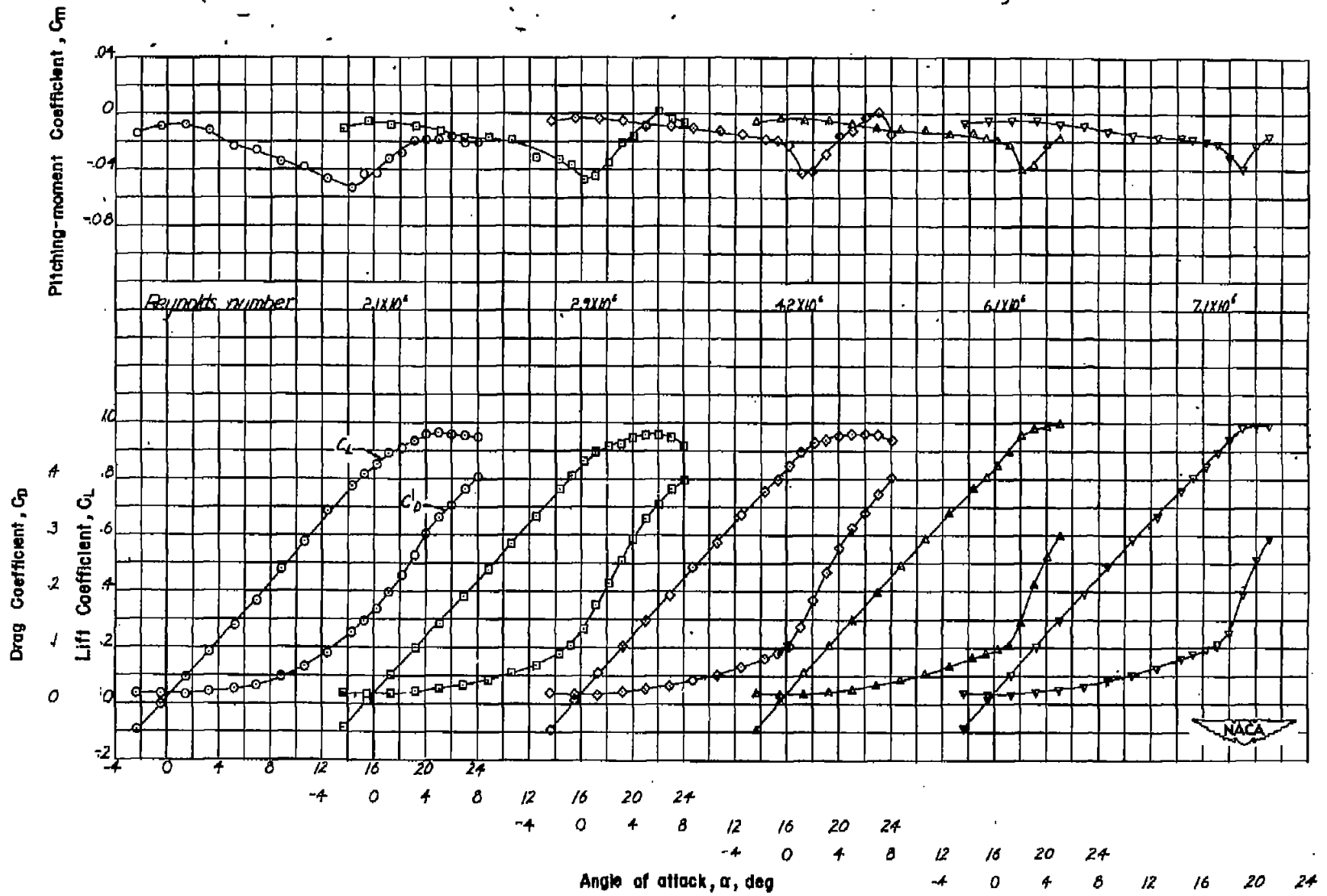


Figure 4.- Schematic drawing of a $47\frac{1}{2}^\circ$ sweptback wing-fuselage combination equipped for boundary-layer control by suction.

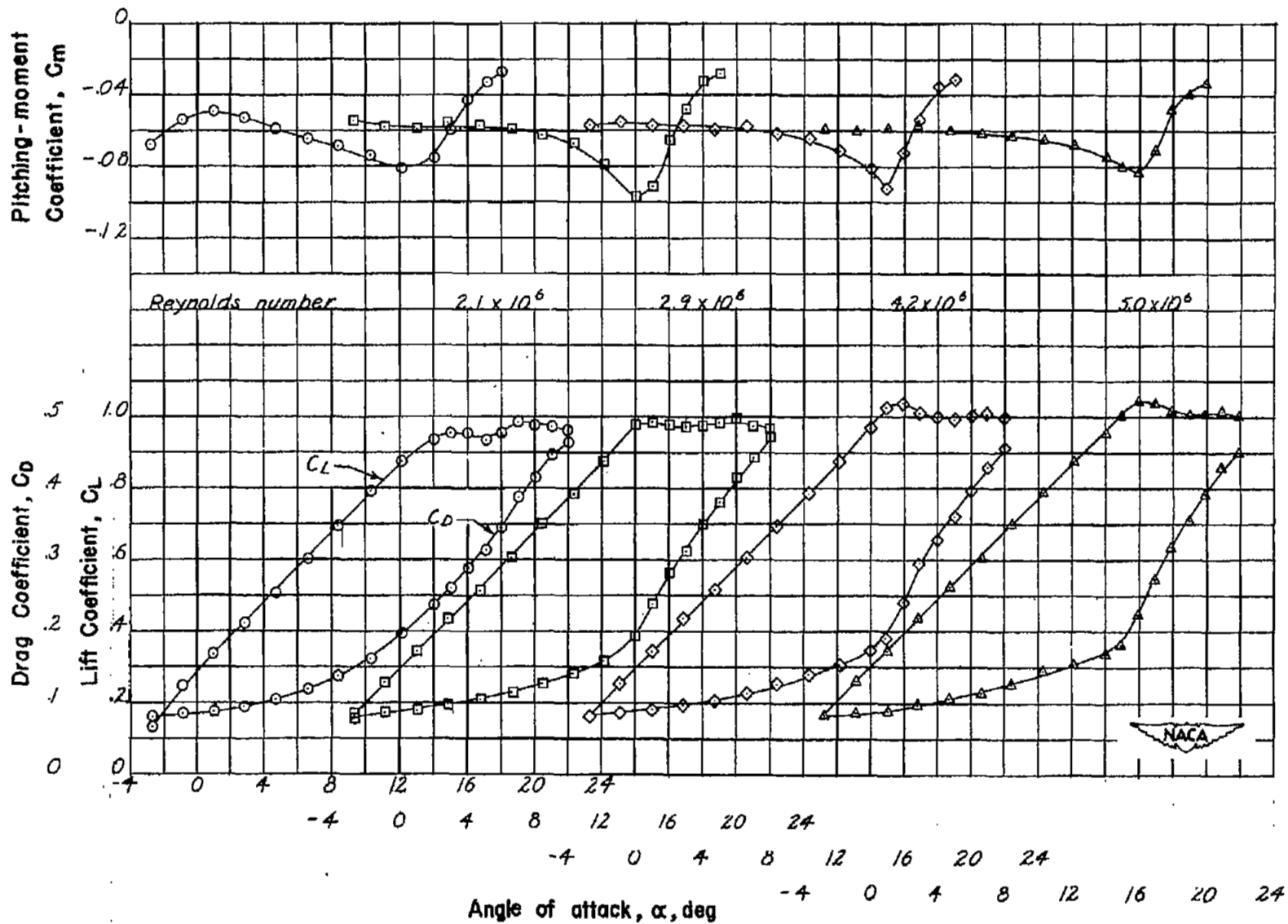






(a) Plain wing.

Figure 5.- Effect of Reynolds number on the aerodynamic characteristics of a 47.5° sweptback wing-fuselage combination with rounded tips. $C_Q = 0$.



(b) Semispan split flaps.

Figure 5.- Concluded.

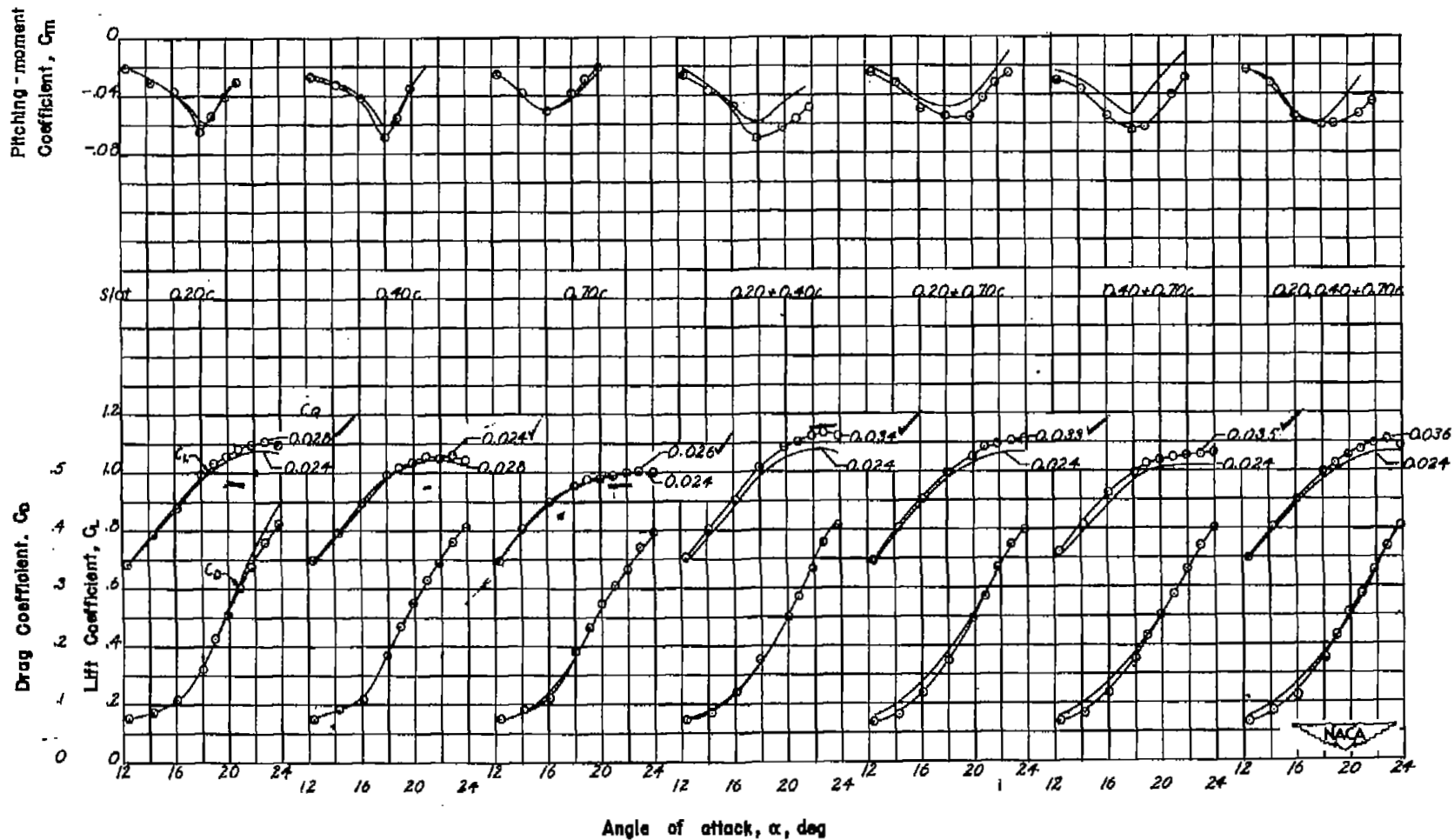


Figure 8.- Effect of slot location on the aerodynamic characteristics of a 47.5° sweptback wing-fuselage combination with boundary-layer control. Plain wing, rounded tips.
 $R = 4.2 \times 10^6$.

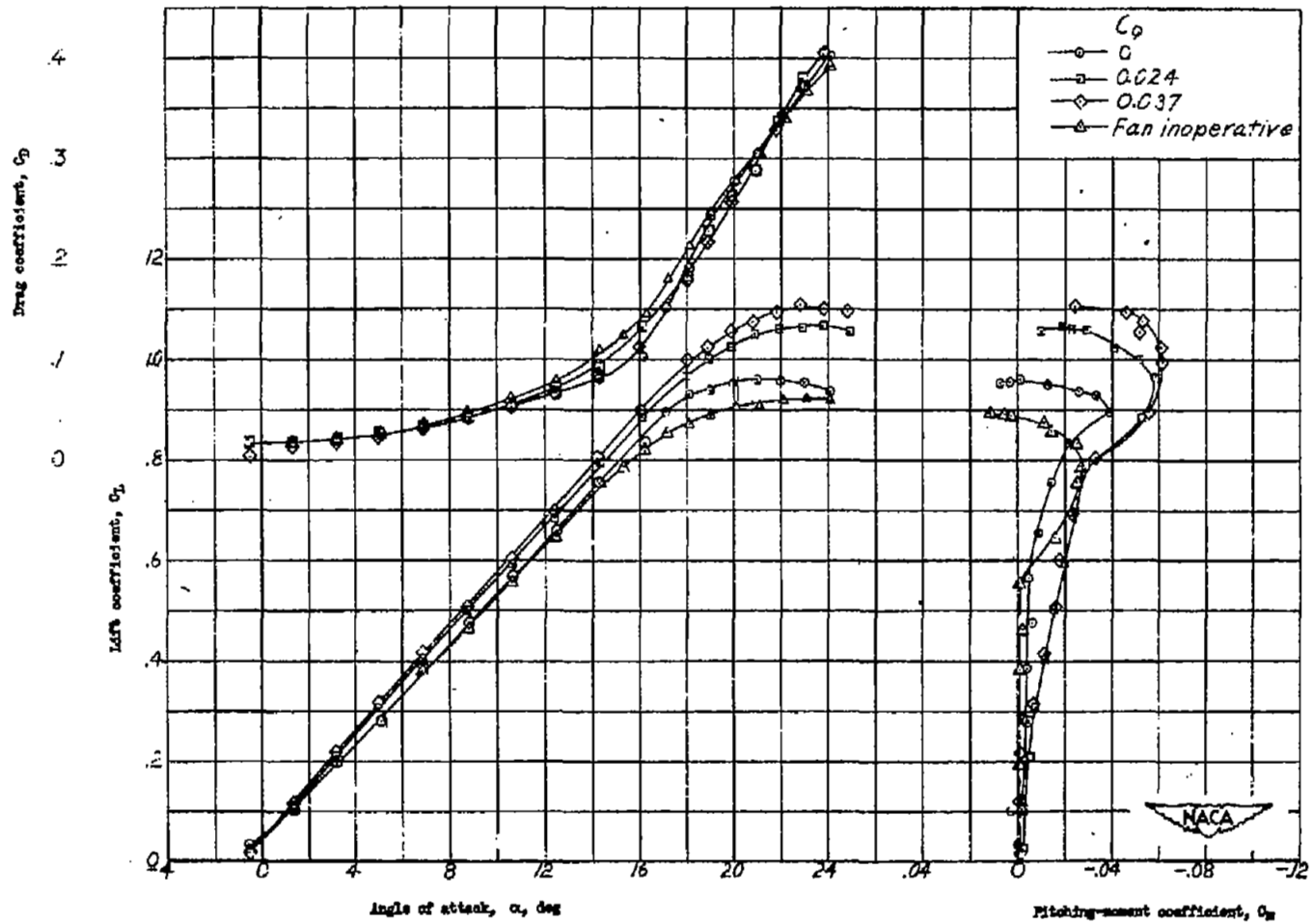


Figure 7.- Effect of boundary-layer control by suction on the aerodynamic characteristics of 47.5° sweptback wing-fuselage combination. Rounded tips. $R = 4.2 \times 10^6$.

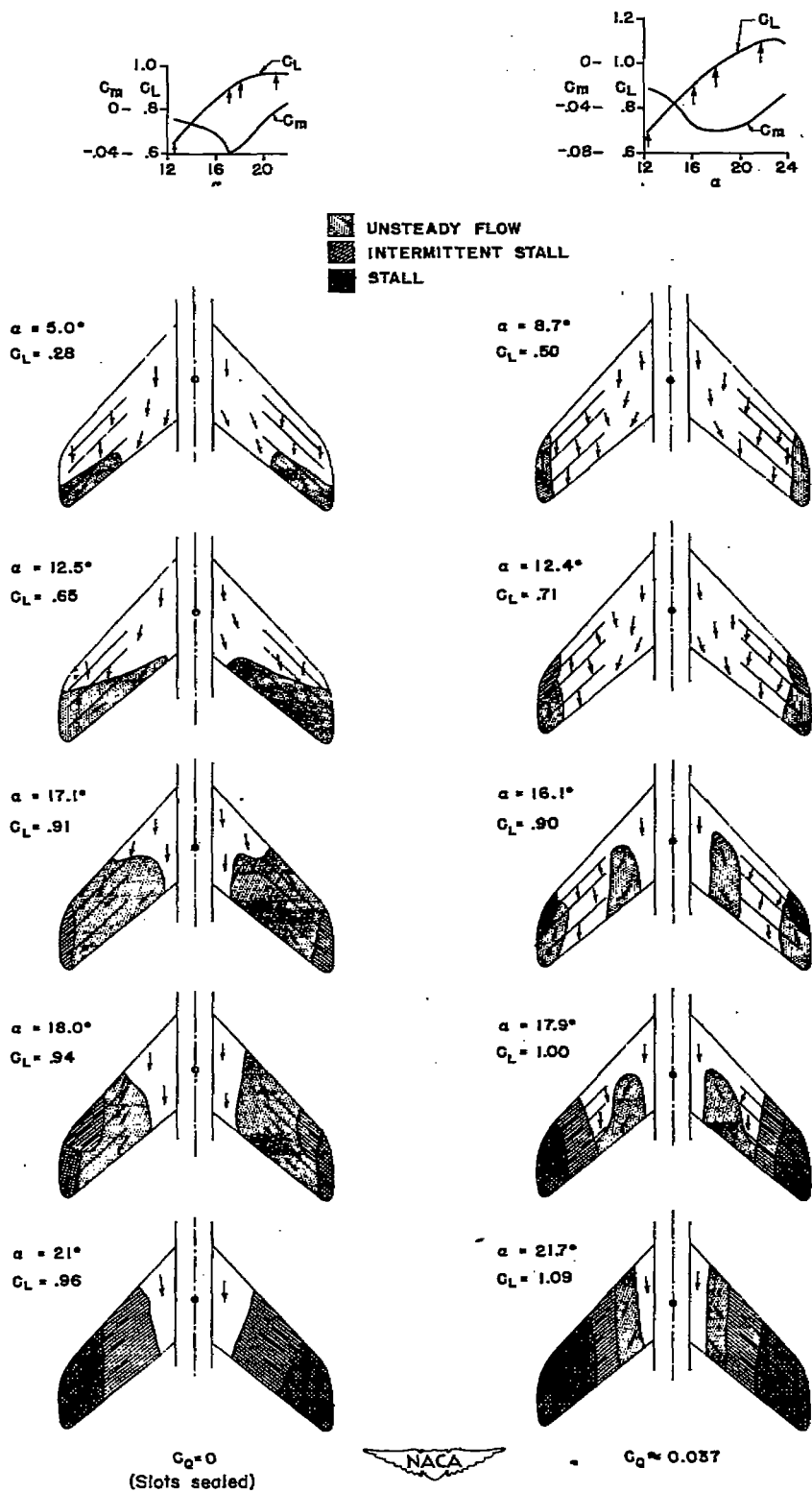
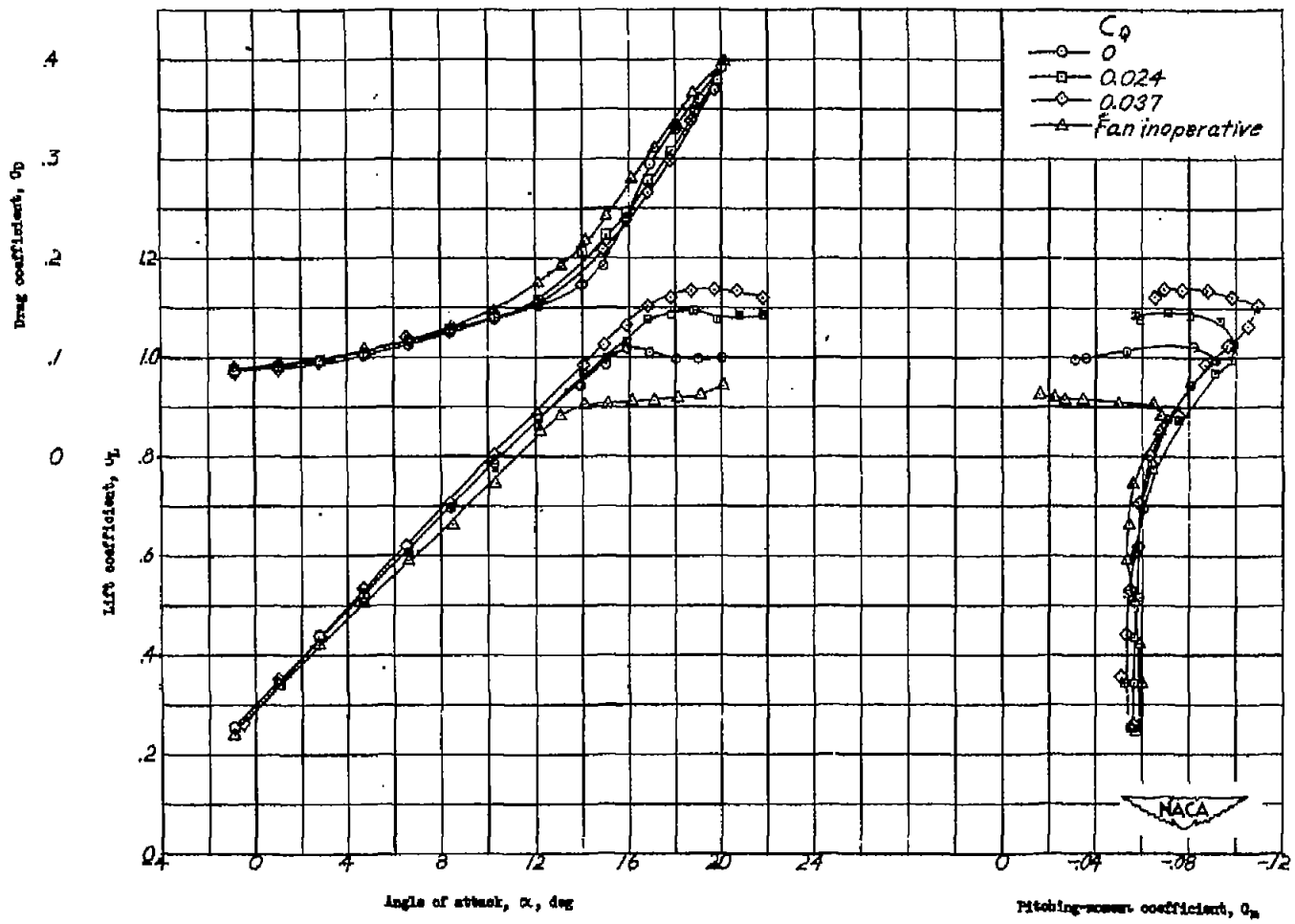
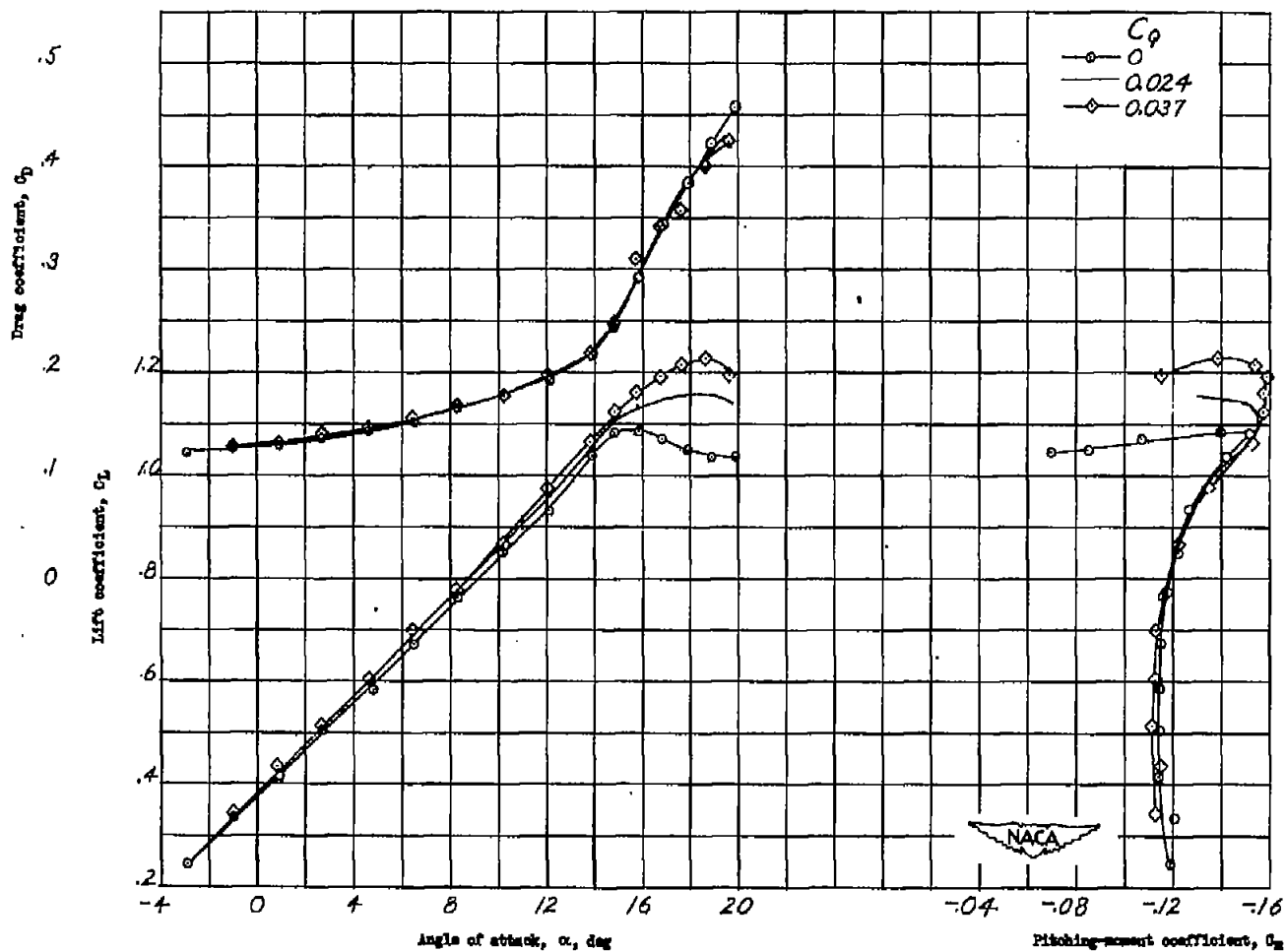


Figure 8.- Stalling characteristics of a 47.5° sweptback wing-fuselage combination with and without suction.



(a) Semispan split flaps.

Figure 9.- Effect of boundary-layer control by suction on the aerodynamic characteristics of 47.5° sweptback wing-fuselage combination with split flaps. Rounded tips. $R = 4.2 \times 10^6$.



(b) Full-span split flaps.

Figure 9.- Concluded.

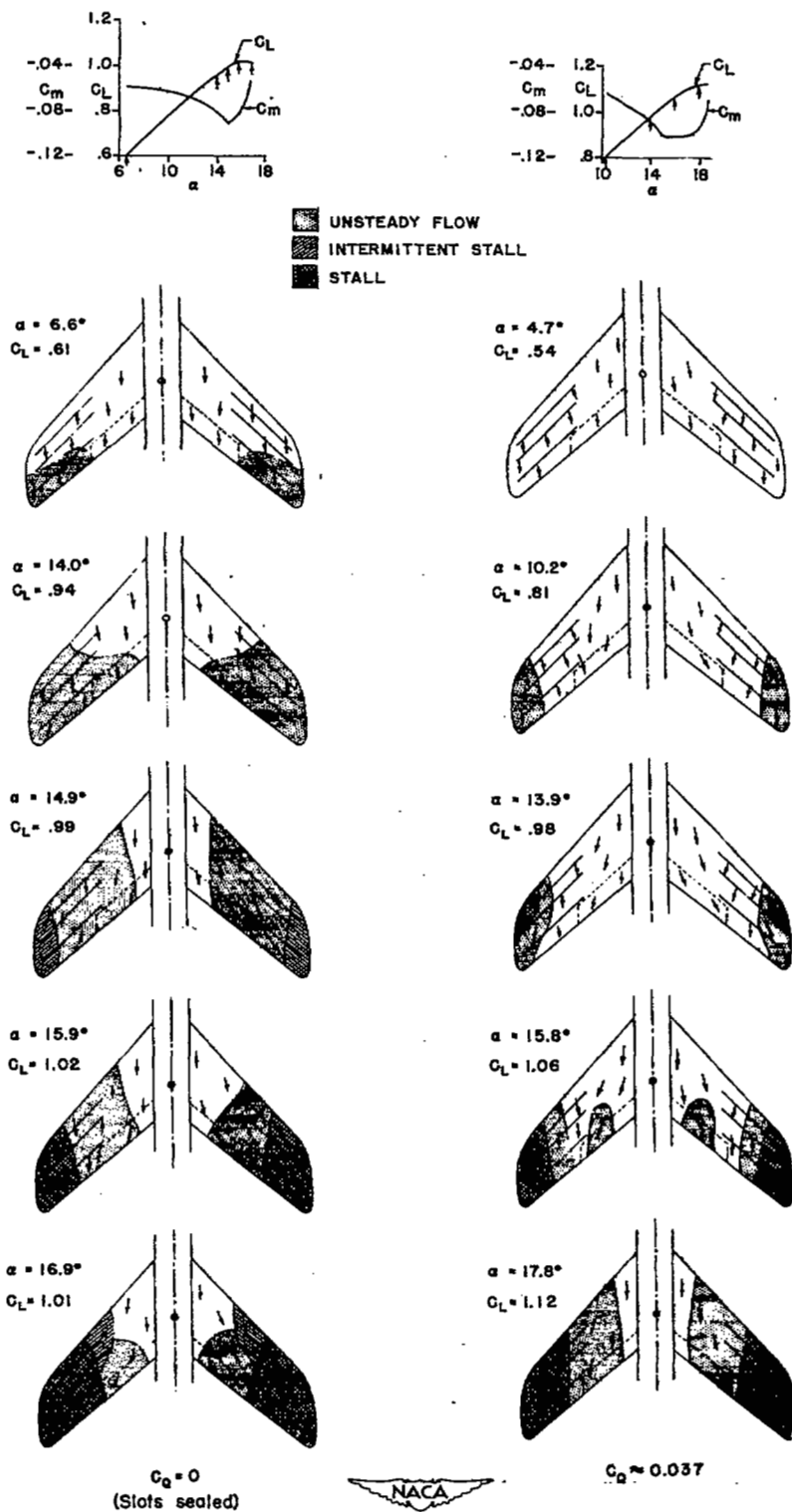
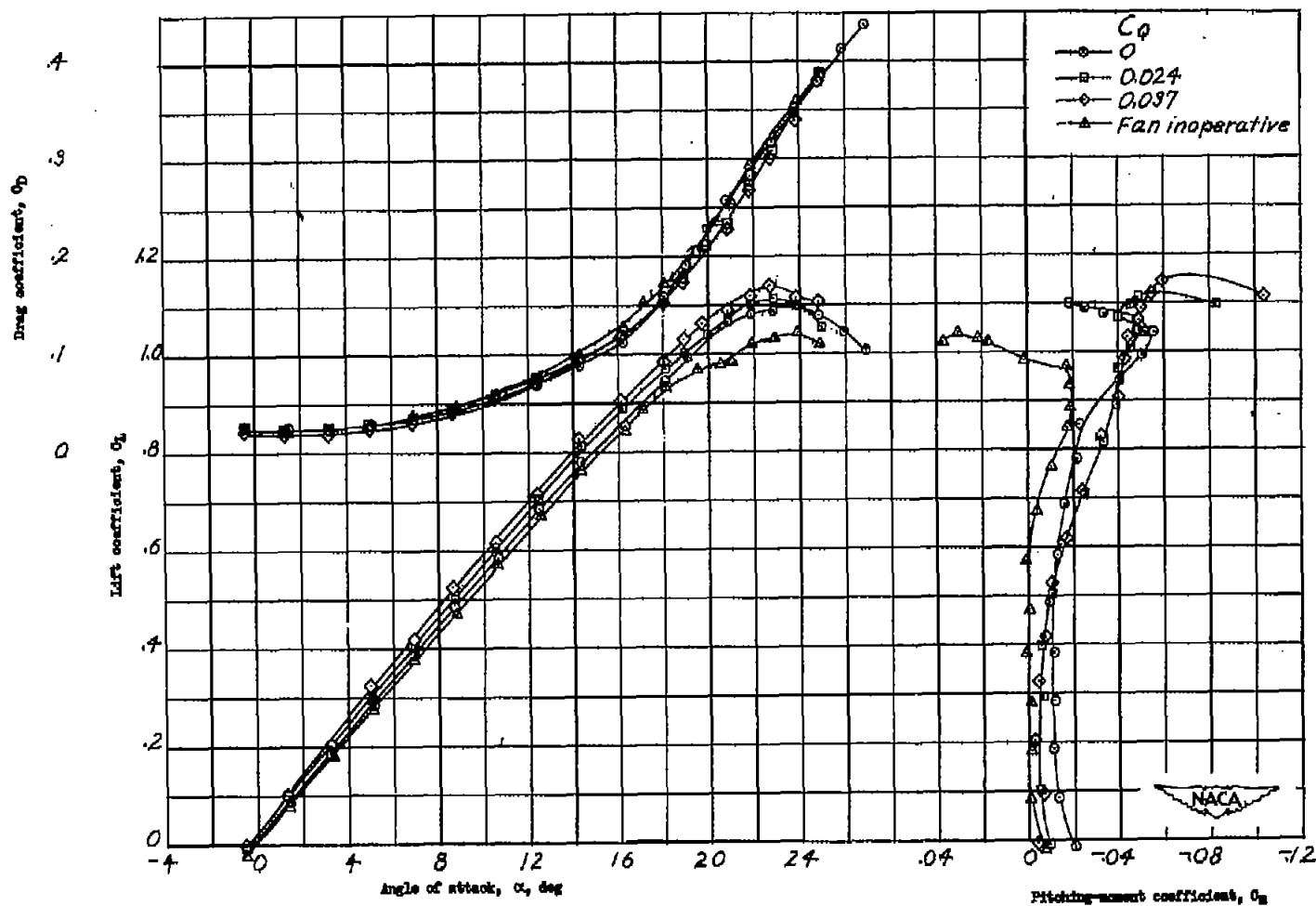
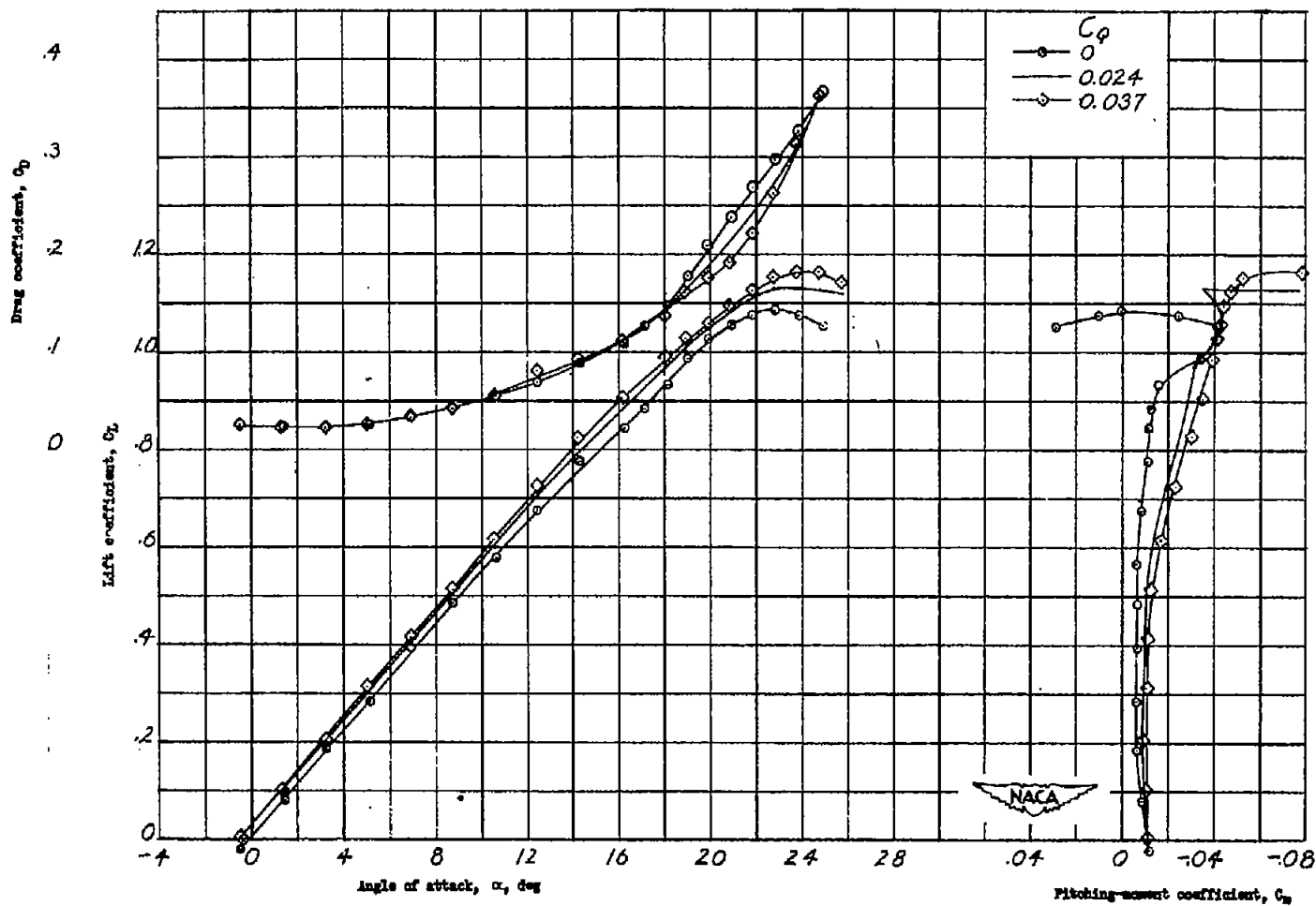


Figure 10.- Effect of semispan split flaps on the stalling characteristics of a 47.5° sweptback wing-fuselage combination with and without suction.



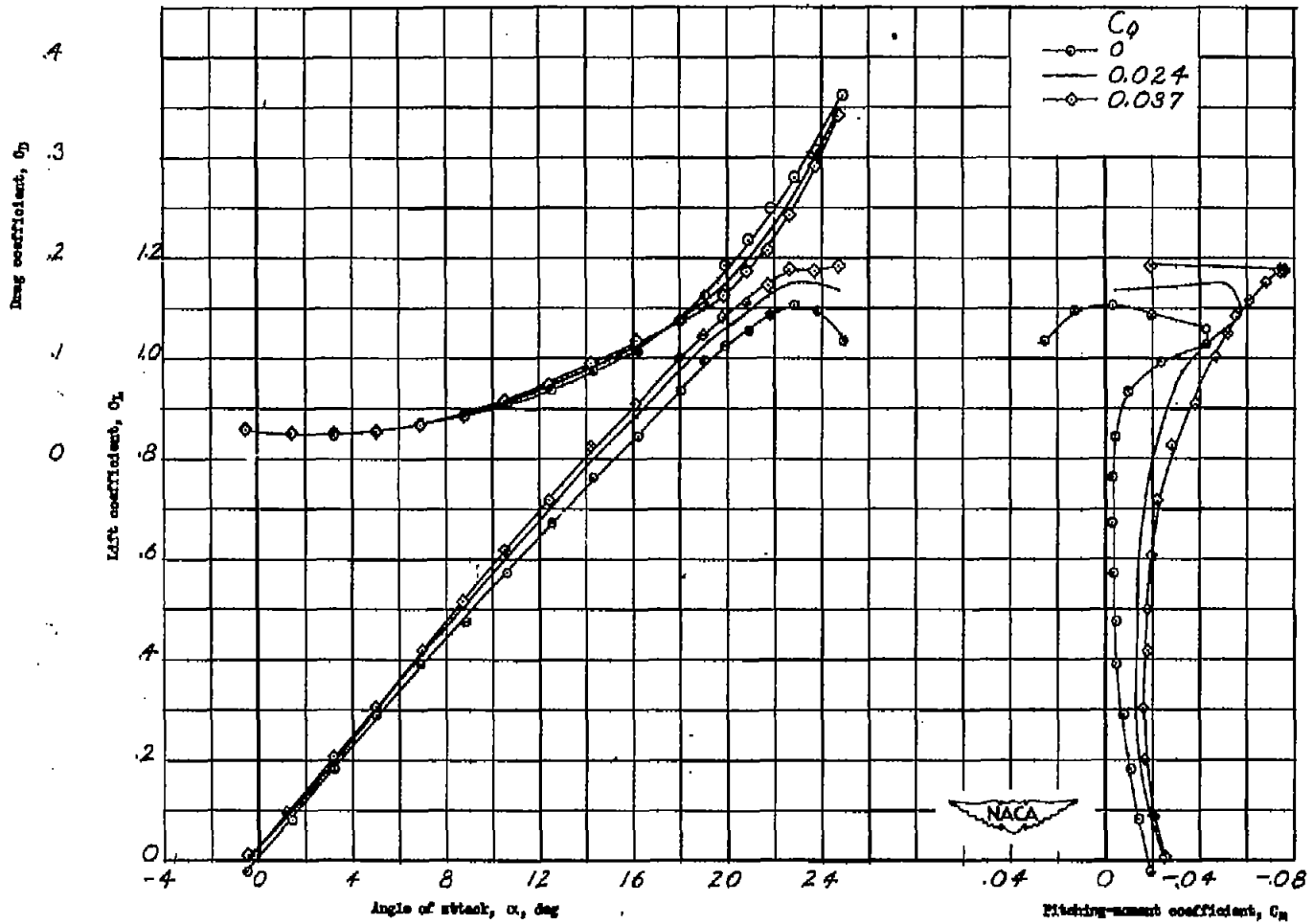
(a) $0.50 \frac{b}{c}$ -span extensible leading-edge flaps.

Figure 11.- Effect of boundary-layer control by suction on aerodynamic characteristics of 47.5° sweptback wing-fuselage combination with extensible leading-edge flaps. Rounded tips. $R = 4.2 \times 10^6$.



(b) $0.60 \frac{b}{2}$ -span extensible leading-edge flaps.

Figure 11.- Continued.



(c) $0.71 \frac{b}{2}$ -span extensible leading-edge flaps.

Figure 11.- Concluded.

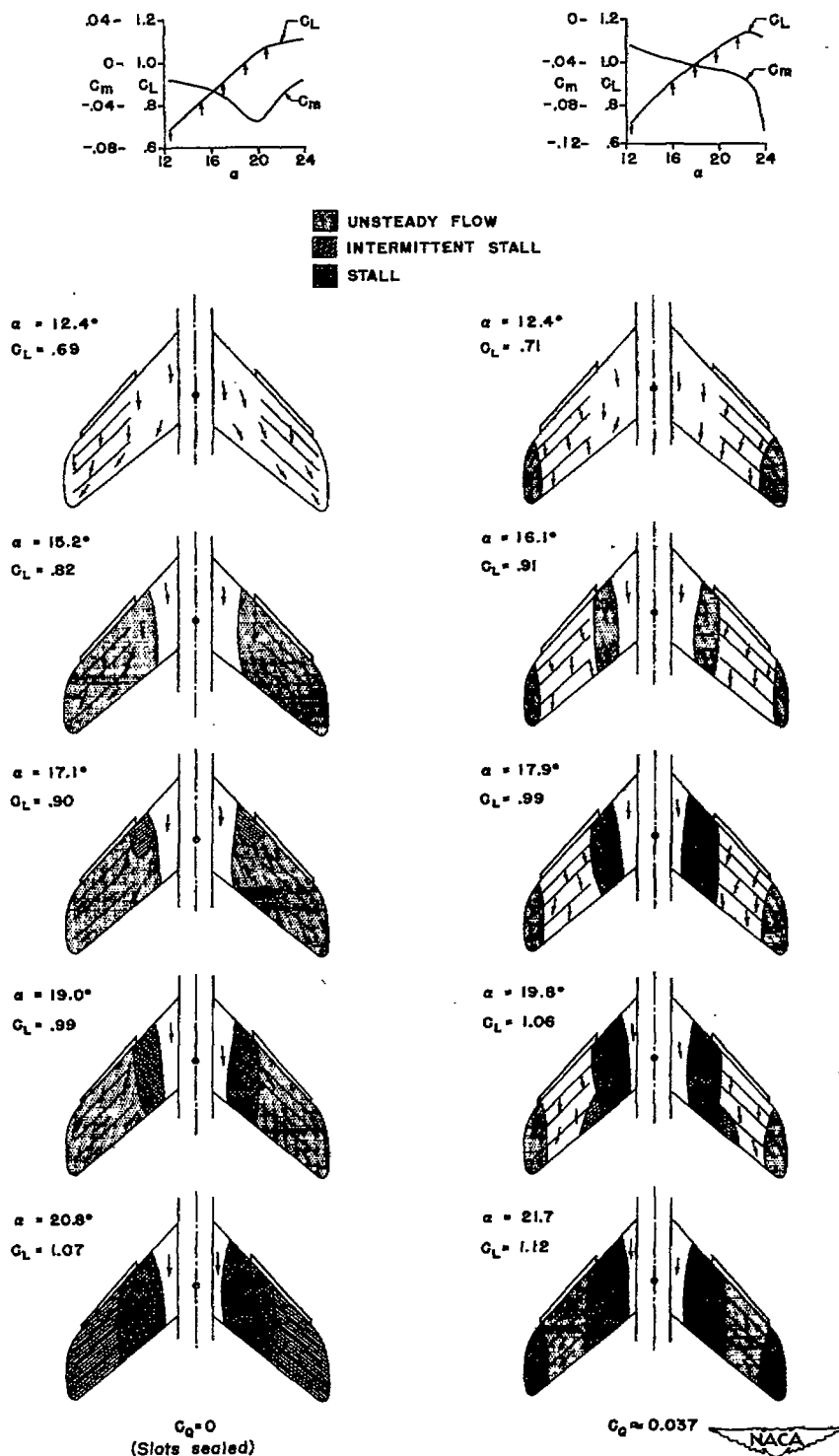
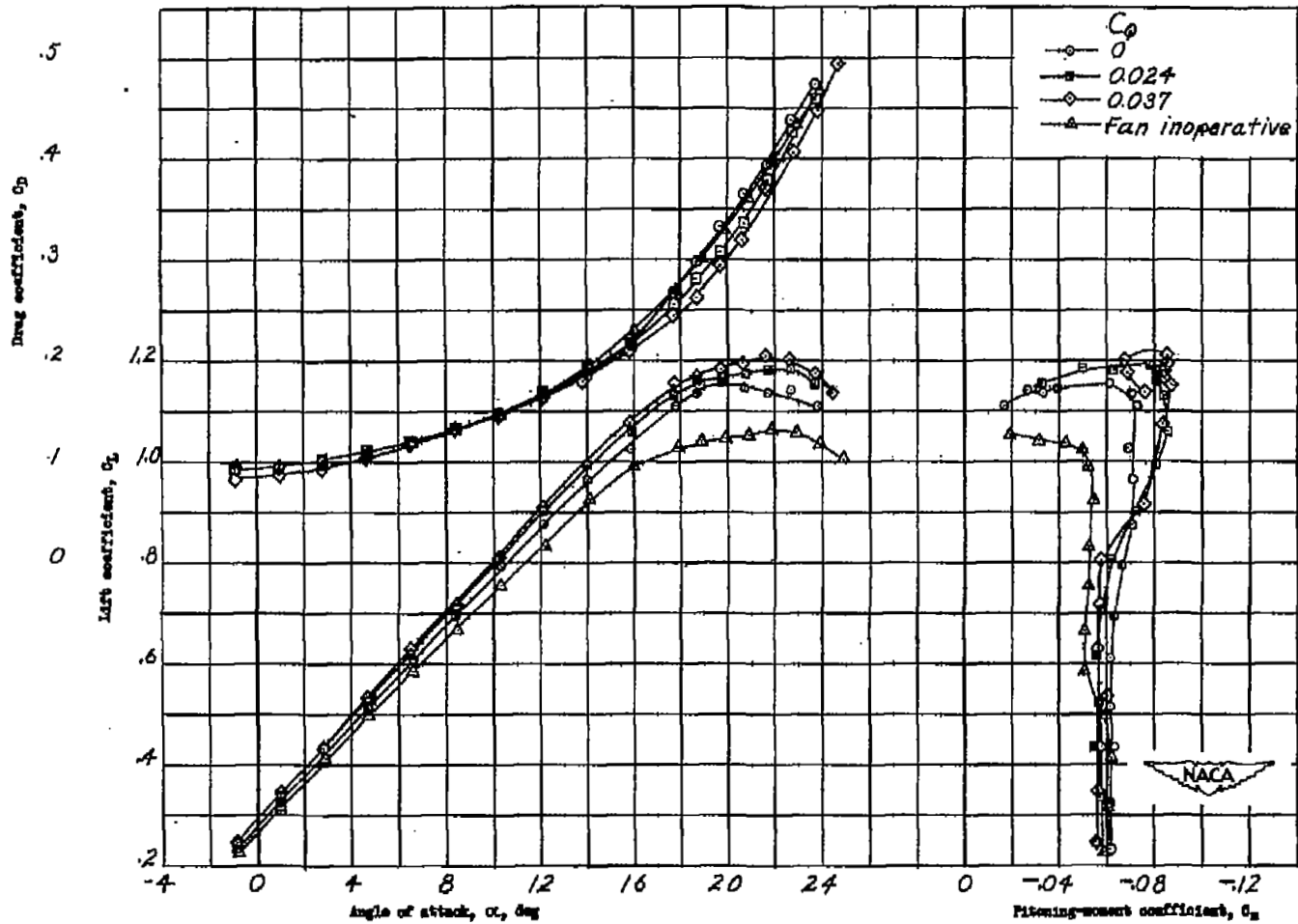
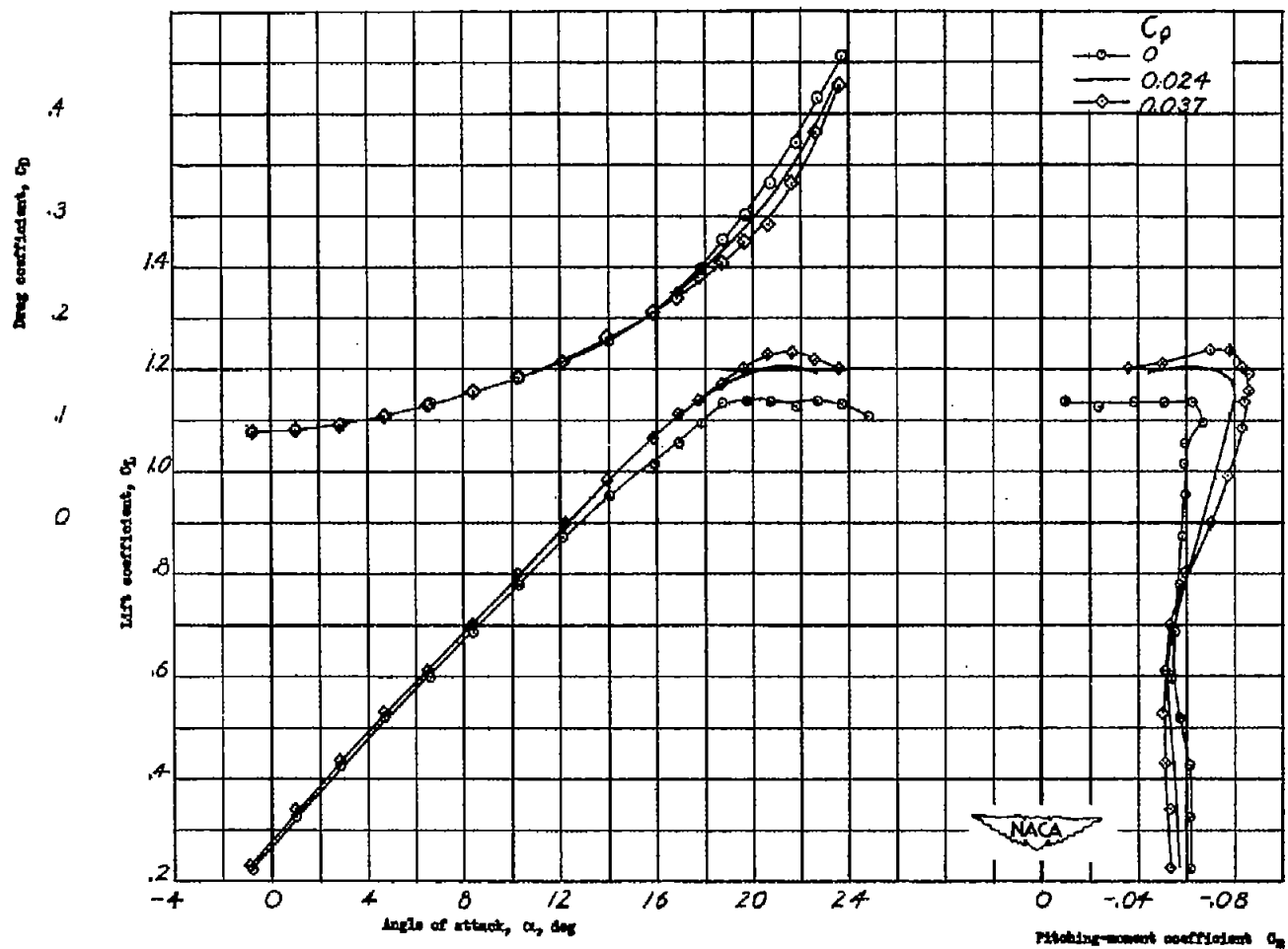


Figure 12.- Effect of $0.50 \frac{b}{2}$ -span extensible leading-edge flaps on the stalling characteristics of a 47.5° sweptback wing-fuselage combination with and without suction.



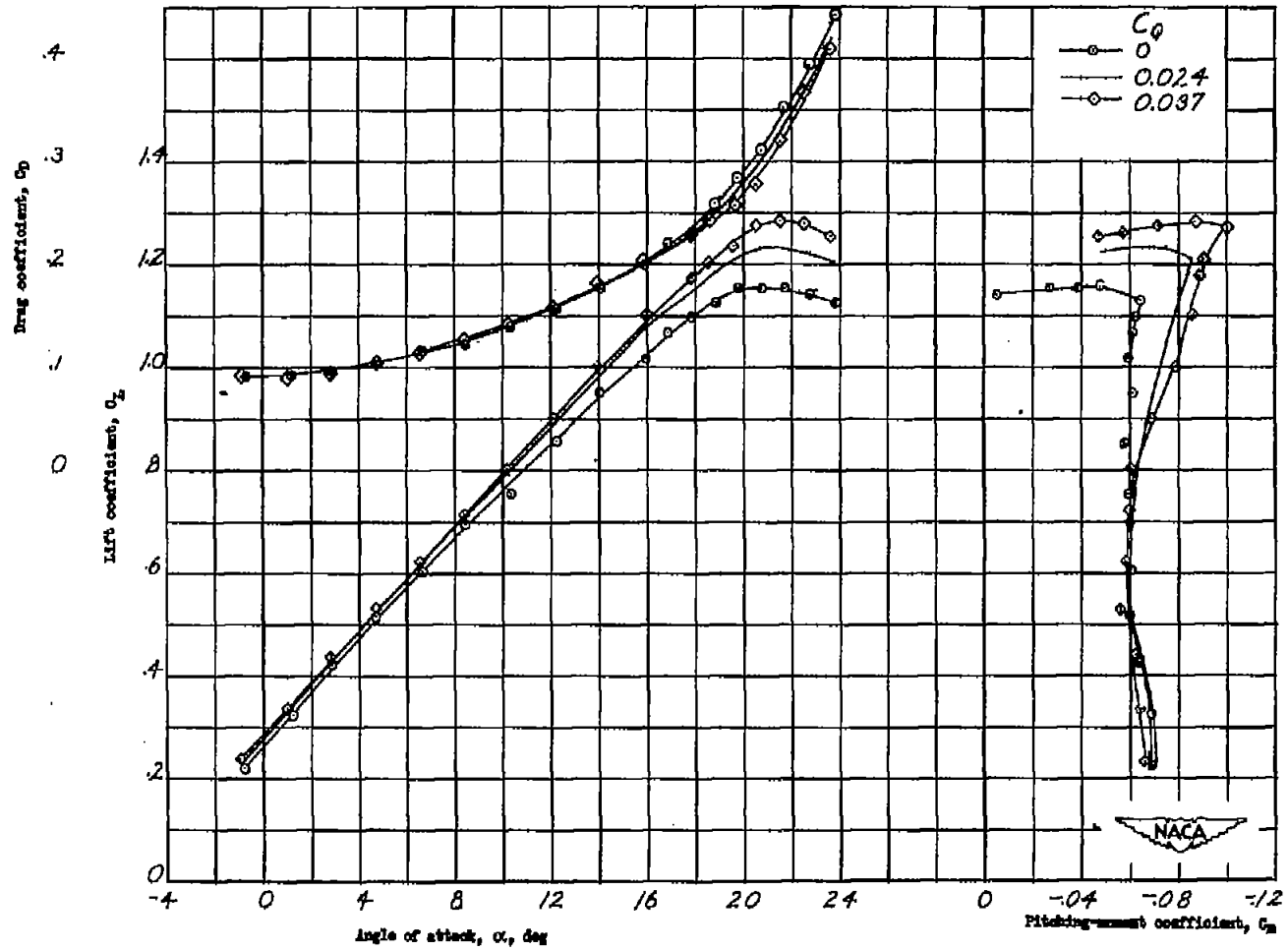
(a) Semispan split flaps and $0.50 \frac{b}{2}$ -span extensible leading-edge flaps.

Figure 13.- Effect of boundary-layer control by suction on aerodynamic characteristics of 47.5° sweptback wing-fuselage combination with split flaps and extensible leading-edge flaps. Rounded tips. $R = 4.2 \times 10^6$.



(b) Semispan split flaps and $0.60 \frac{b}{2}$ -span extensible leading-edge flaps.

Figure 13.- Continued.



(c) Semispan split flaps and $0.71 \frac{b}{2}$ -span extensible leading-edge flaps.

Figure 13.- Concluded.

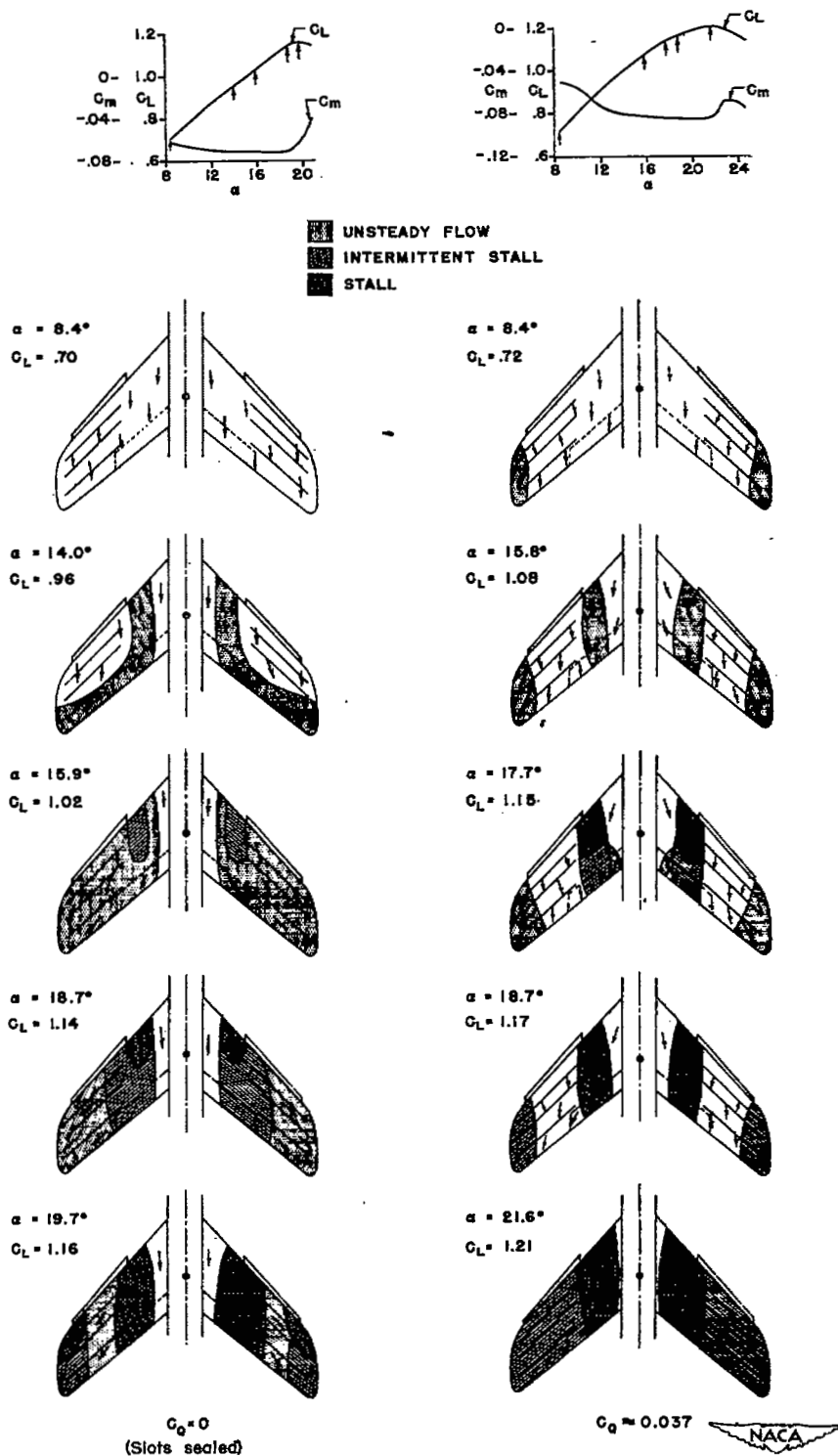


Figure 14.- Effect of semispan split flaps and $0.50 \frac{b}{2}$ -span extensible leading-edge flaps on the stalling characteristics of a 47.5° swept-back wing-fuselage combination with and without suction.

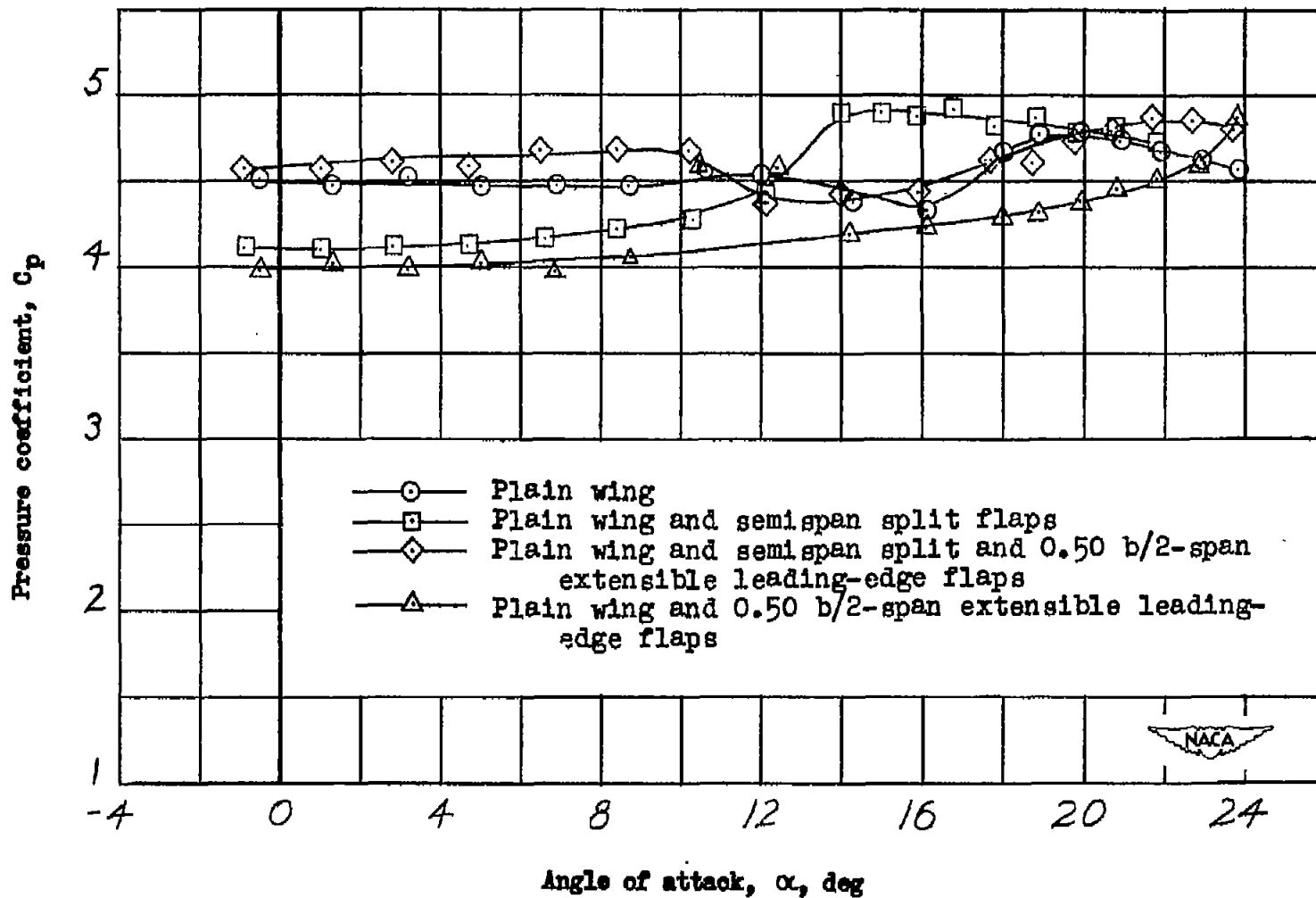
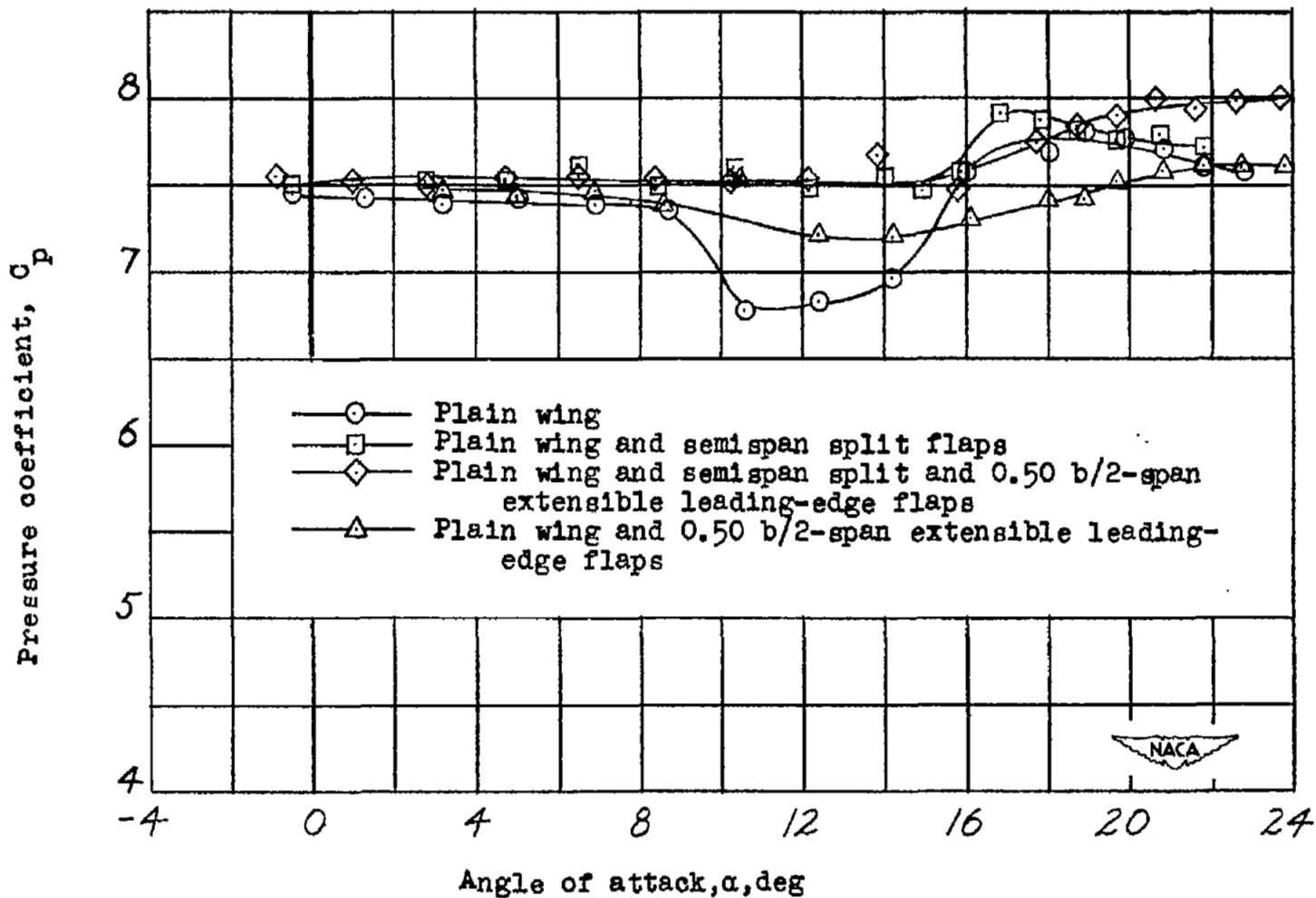
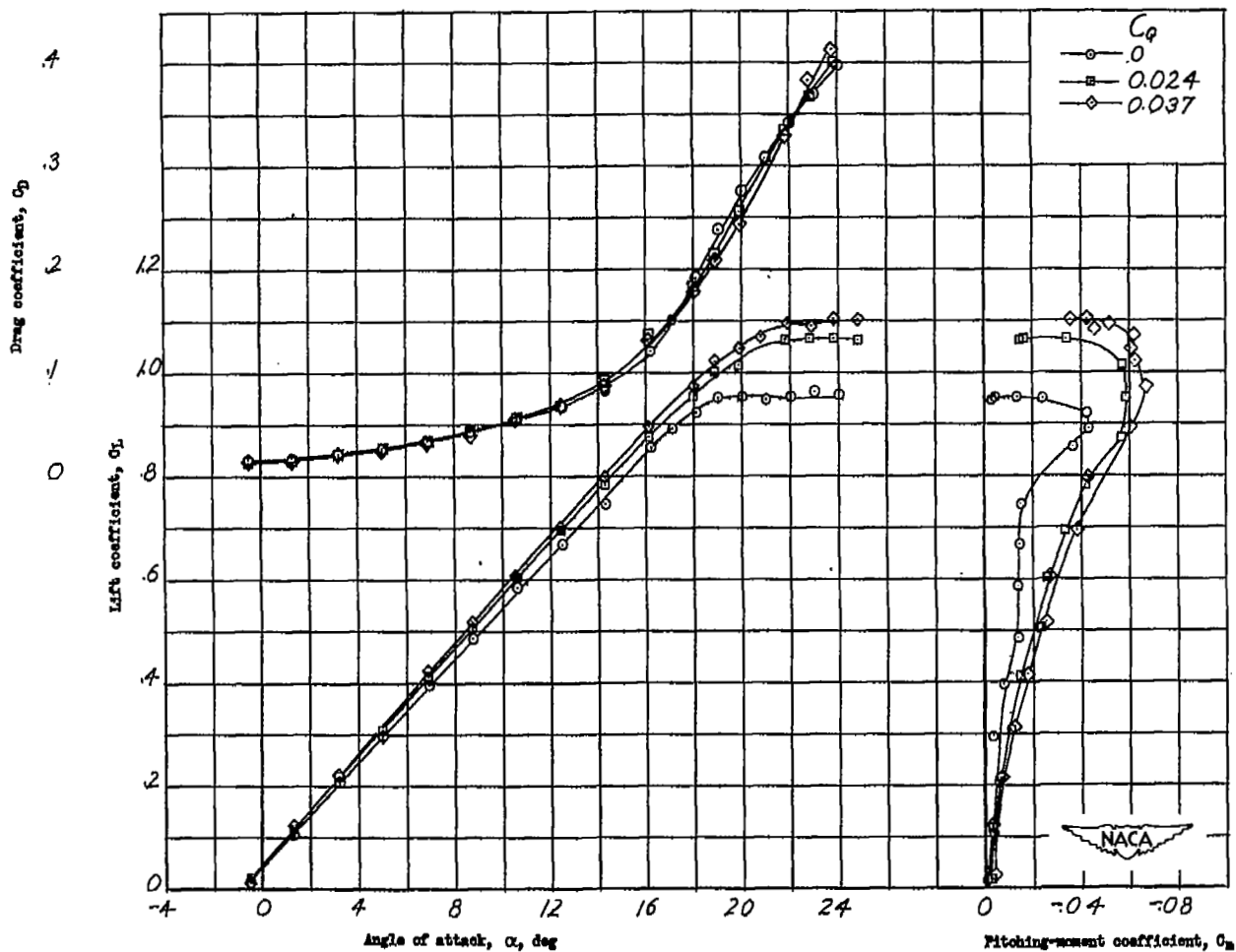
(a) $C_Q = 0.024$.

Figure 15.- Variation of pressure coefficient with angle of attack for 47.5° sweptback wing-fuselage combination with boundary-layer control by suction. Rounded tips.



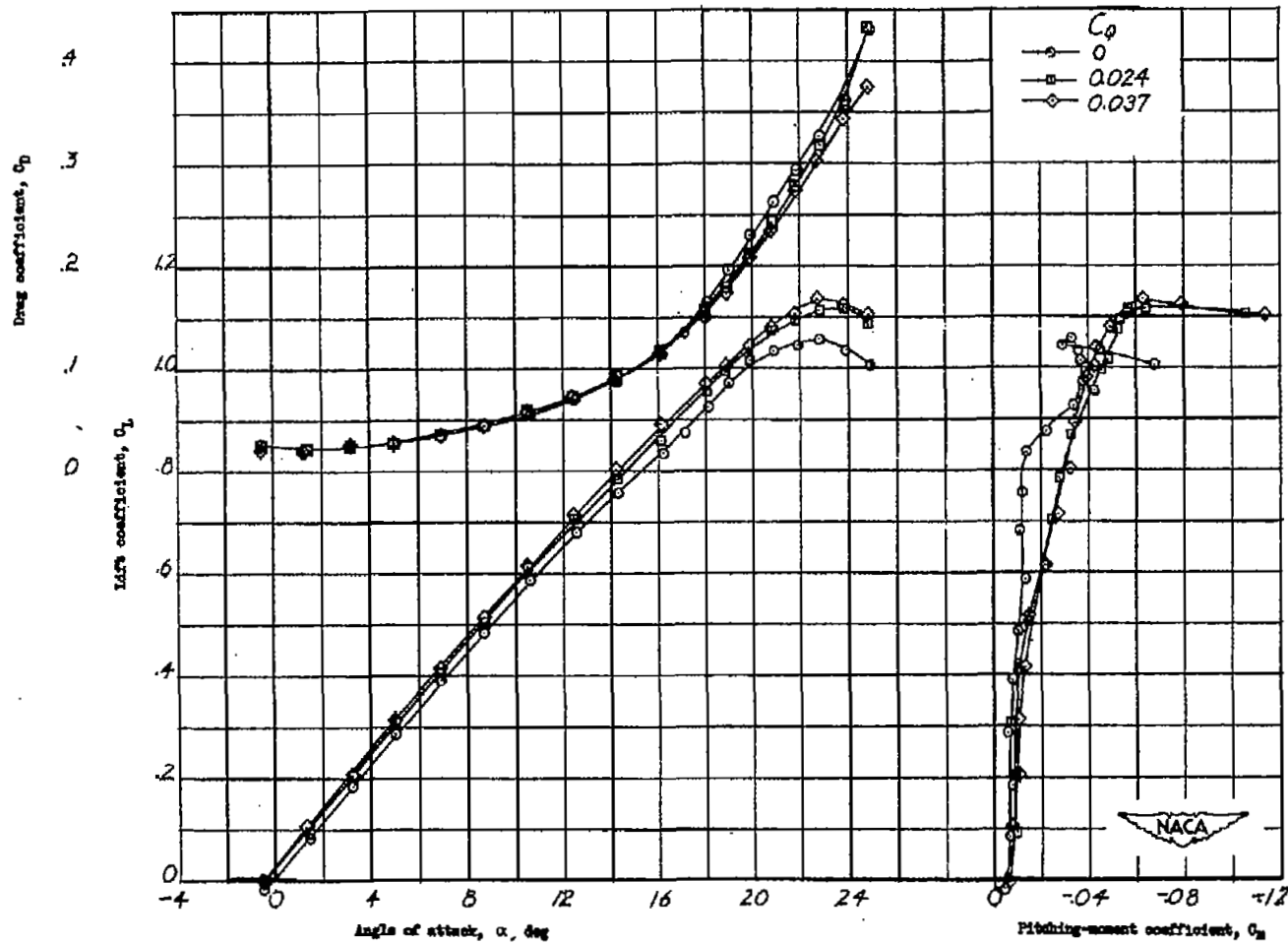
(b) $C_Q = 0.037$.

Figure 15.- Concluded.



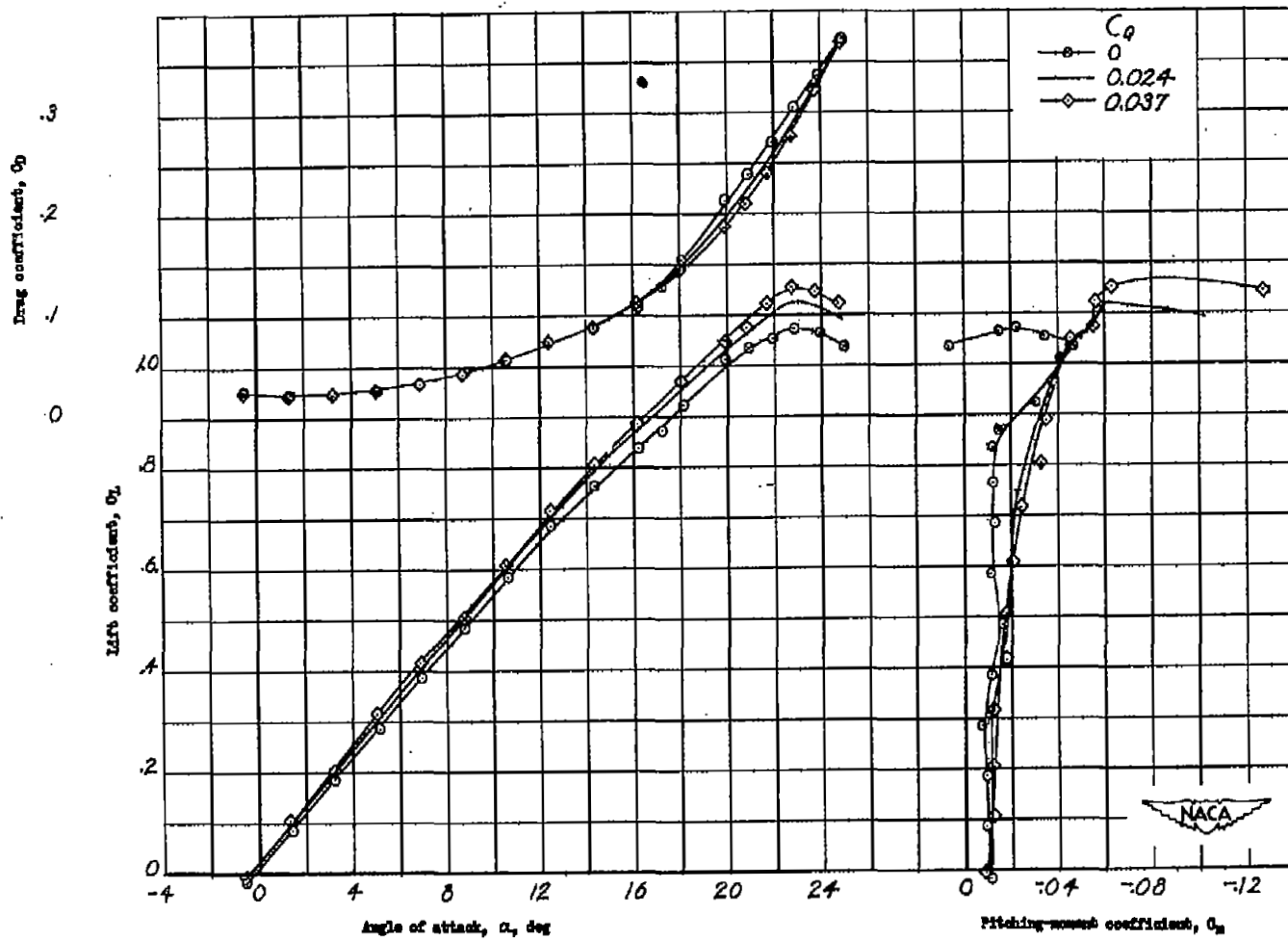
(a) Plain wing.

Figure 16.- Effect of boundary-layer control by suction on aerodynamic characteristics of 47.5° sweptback wing-fuselage combination. Square tips. $R = 4.2 \times 10^6$.



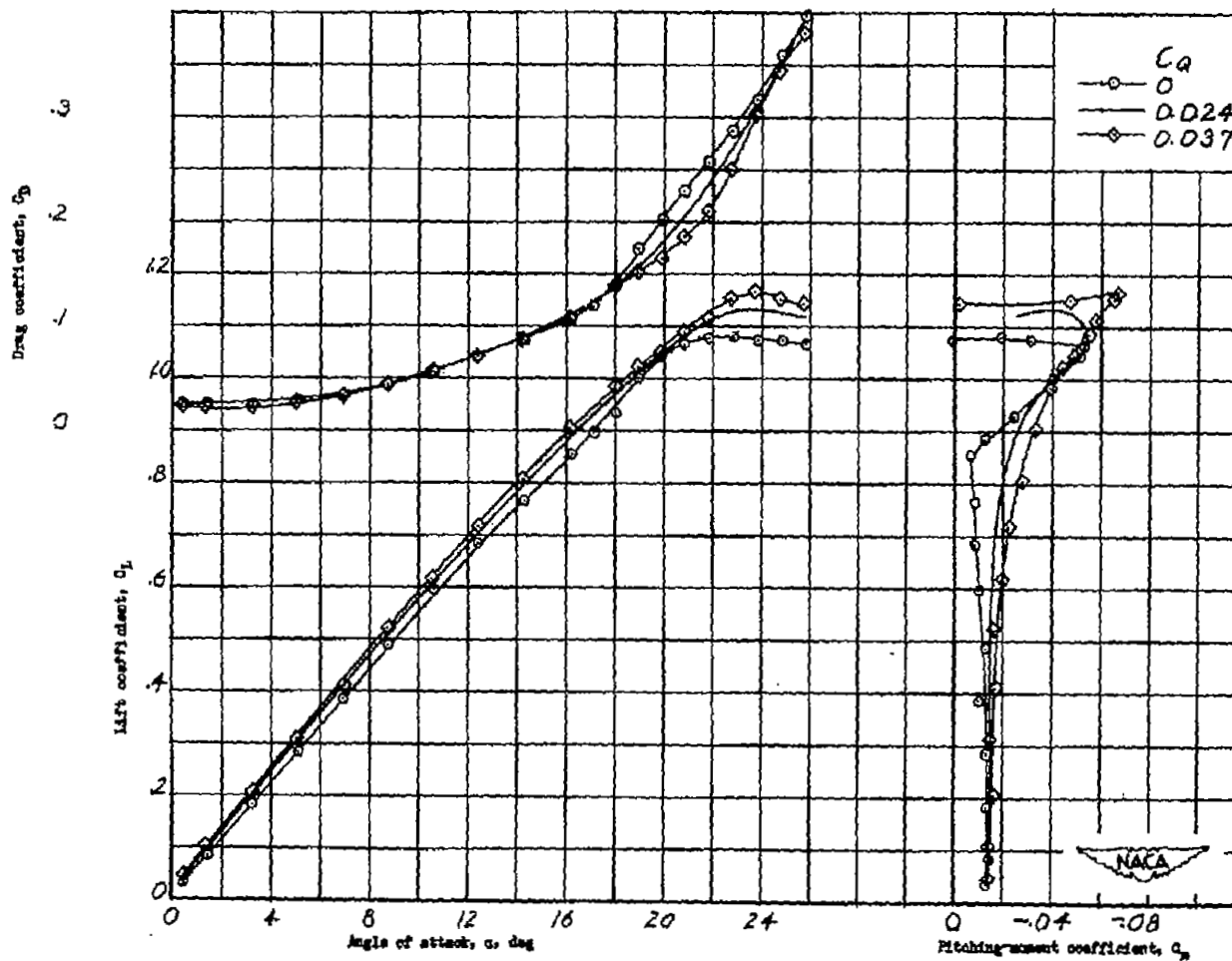
(b) $0.50 \frac{b}{2}$ -span extensible leading-edge flaps.

Figure 16.- Continued.



(c) $0.60 \frac{b}{2}$ -span extensible leading-edge flaps.

Figure 16.- Continued.



(d) $0.71 \frac{b}{2}$ -span extensible leading-edge flaps.

Figure 18.- Concluded.